DEPARTAMENTO DE CIÊNCIAS DA VIDA

FACULDADE DE CIÊNCIAS E TECNOLOGIA
UNIVERSIDADE DE COIMBRA

MiRNA contribution to APP metabolism and Aβ production in Alzheimer's disease:

Identification of new miRNA-related SNPs in the 3'UTR of human APP and ApoE genes

Ricardo Jorge Carreira da Silva

2013

DEPARTAMENTO DE CIÊNCIAS DA VIDA

FACULDADE DE CIÊNCIAS E TECNOLOGIA
UNIVERSIDADE DE COIMBRA

MiRNA contribution to APP metabolism and Aβ production in Alzheimer's disease:

Identification of new miRNA-related SNPs in the 3'UTR of human APP and ApoE genes

Ricardo Jorge Carreira da Silva

2013

"All of science is nothing more than the refinement of everyday thinking"

Albert Einstein

"Physics and Reality"

(1936)

Agradecimentos

MiRNA contribution to APP metabolism and Aβ production in Alzheimer's disease: Identification of new miRNA-related SNPs in the 3'UTR of human APP and APOE genes

II

Table of contents

MiRNA contribution to APP metabolism and Aβ production in Alzheimer's disease:
Identification of new miRNA-related SNPs in the 3'UTR of human APP and APOE genes

IV

Abbreviations

3'UTR – 3'untranslated region

Aβ – Amyloid beta

Aβ42 – amyloid peptide 42

ABCA-1 - ATP-binding cassette transporter 1

AD – Alzheimer's Disease

AICD – APP intracellular domain

APP – Amyloid precursor protein

Bace1 - Beta-secretase 1

CDK5 –Cyclin dependant kinase 5

cKO – Conditional Knock-out

CNS – Central nervous system

CPS – Counts per second

DMEM - Dulbecco's Modified Eagle Medium

DNA - Deoxyribonucleic acid

dNTP - Deoxyribonucleotide

EDTA - Ethylenediaminetetraacetic acid

Fw - Forward

GFP – Green fluorescent protein

GSK3β – Glycose synthase kinase 3 beta

HDL –High density lipoproteins

MiRNA contribution to APP metabolism and Aβ production in Alzheimer's disease:
Identification of new miRNA-related SNPs in the 3'UTR of human APP and APOE genes

v

HEK – Human embryonic kidney

LB - Lysogeny broth

LDL – Low density pipoprotein

LTP – Long-term potentiation

MCI – Mild cognitive impairment

miRNA – Micro Ribonucleic acid

mRNA – Messenger Ribonucleic acid

nts - Nucleotides

OPTIMEM - modification of Eagle's Minimum Essential Media

PSEN-1 – Presenilin 1

Re – Reverse

RISC - RNA-induced silencing complex

RNA - Ribonucleic acid

SNP – Singular nucleotide polymorphism

SOC - Super Optimal broth with Catabolite repression

UV – Ultra-violet

MiRNA contribution to APP metabolism and Aβ production in Alzheimer's disease:
Identification of new miRNA-related SNPs in the 3'UTR of human APP and APOE genes

VI

Abstract

Alzheimer's disease (AD) is a severe neurodegenerative disorder, characterized by the accumulation of β-amyloid plaques in the extracellular space and an excessive phosphorilation of neuronal Tau. Both these factors are believed to be intimately related with the neuronal loss and inflammation observed in this pathology.

Although AD can be considered a sporadic disease associated with the aging process, a small percentage of AD cases have been associated with specific gene mutations and/or duplications, emphasizing the importance of the deregulation of protein expression in this pathology.

MicroRNAs are conserved small non-coding RNAs that control gene expression at the posttranscriptional level and are, thus, essential to ensure proper cellular function. Alzheimer's disease profiling experiments have shown that several microRNAs are implicated in the regulation of key genes involved in the amyloidogenic pathway (such as APP, BACE1 and MAPT), suggesting that miRNA deregulation can contribute to the progression of this disease

The present study aims to unravel the role of microRNAs as posttranscriptional regulators in AD, evaluating how single nucleotide polymorphisms (SNPs) present in the 3'UTR of two AD-related genes (APP and ApoE) can influence miRNA binding and, consequently, APP and ApoE expression.

Using a gene sequencing technique based on the Sanger method, we were able to identify and validate a heterozygous SNP in the 3'UTR region of the APP gene, which may contribute to AD onset and development. Our results suggest that the presence of this SNP can interfere with the binding of several miRNAs to the mRNA of APP, promoting APP upregulation and the consequent increase of Aβ deposition in the nervous tissue. In addition, using a luciferase-based assay, we were able to provide evidence that miRNA-485-5p is capable of regulating APP expression at the posttranscriptional level, by binding to the 3'UTR of APP mRNA, thus validating APP as a direct target of this miRNA..

Taken together, our results highlighted the effects of miRNA-related genetic variations in the etiopathology of AD and suggest that miRNA-485-5p can be a new and interesting therapeutic target for this disease.

MiRNA contribution to APP metabolism and Aβ production in Alzheimer's disease: Identification of new miRNA-related SNPs in the 3'UTR of human APP and APOE genes

VII

Resumo

A doença de Alzheimer é uma patologia neurodegenerativa grave, caracterizada pela acumulação extracelular de placas do péptido β-amilóide e por uma fosforilação excessiva da proteína Tau. Ambos estes factores aparentam estar intimamente relacionados com a perda neuronal e inflamação que são verificadas nesta doença.

Apesar de a doença de Alzheimer poder ser considerada uma doença esporádica, associada ao envelhecimento, uma pequena percentagem dos casos diagnosticados estão associados a mutações ou duplicações de genes específicos, dando ênfase à importância que a desregulação da expressão proteica pode desempenhar nesta patologia.

Os microRNAs sao pequenos RNAs não codificantes que regulam a expressão génica ao nível pós-transcripcional, sendo assim fundamentais para o desempenho eficaz das funções celulares.

Estudos do perfil de microRNAs, no contexto da doença de Alzheimer, permitiram indentificar vários microRNAs implicados na regulação de genes envolvidos no desencadeamento da cascata amiloidogénica (tais como os genes da APP, BACE1 e MAPT), reforçando a ideia de que os microRNAs podem contribuir para a progressão desta doença.

O prsente estudo procura esclarecer o papel dos microRNAs como reguladores pós-transcripcionais na doença de Alzheimer, avaliando de que forma a presença de polimorfismos na sequência de nucleótidos da região 3'UTR de dois genes implicados nesta doença (APP e ApoE) pode influenciar a ligação de microRNAs a esta região e, consequentemente, afectar a expressão destes mesmos genes.

Usando uma técnica de sequenciação baseada no método de *Sanger*, identificámos e validámos a presença de um polimorfismo heterozigótico na região 3'UTR do gene da APP, que pode contribuir para incidência e desenvolvimento da doença de Alzheimer. Os nossos resultados sugerem que a presença deste polimorfismo pode interferir com a ligação de vários microRNAs ao RNA mensageiro da APP, promovendo assim a produção do peptídeo precursor amilóide e aumentando a deposição de placas senis no tecido nervoso. Através de um ensaio baseado na

MiRNA contribution to APP metabolism and Aβ production in Alzheimer's disease: Identification of new miRNA-related SNPs in the 3'UTR of human APP and APOE genes

VIII

expressão de luciferase, demonstrámos também que o microRNA-485-5p é capaz de regular a expressão da APP através da ligação á região 3'UTR do RNA mensageiro, validando assim o RNA mensageiro desta proteína, validando-a assim como um alvo directo deste microRNA.

Em conjunto, estes resultados realçam os efeitos que as variações genéticas relacionadas com os microRNAs podem causar na incidência e desenvolvimento da doença de Alzheimer e sugerem que o microRNA-485-5p pode providenciar um novo e interessante alvo terapêutico para esta doença.

Palavras-chave: Peptídeo precursor amilóide, Apolipoproteína E, 3'UTR, Alzheimer

MiRNA contribution to APP metabolism and Aβ production in Alzheimer's disease:
Identification of new miRNA-related SNPs in the 3'UTR of human APP and APOE genes

IX

Introduction

1. Introduction

With the current worldwide aging demography there is an increasing toll on health care costs and population's life quality due to a higher incidence of age-related clinical conditions, such as dementia[1,2].

Dementia is a clinical syndrome defined by the constant decline of an individual's cognitive abilities such as memory, language, logic thinking and spatial orientation. [1,3].

When a diagnosed case of dementia is coincident with abnormal accumulation in the brain of insoluble aggregates of both amyloid plaques (also known as senile plaques) and neurofibrillary tangles it is referred to as a case of Alzheimer's Disease[4] [1]. Alzheimer's disease accounts for over 60% of all cases of dementia worldwide. [1,5]. However, the accumulation of this non-soluble protein aggregates can also be found in brains of patients suffering from other neurodegenerative diseases and even in patients without any history of neurological pathology. Therefore, by themselves, these structures cannot account for all the clinical symptoms of AD, suggesting the contribution of additional factors to the full development and establishment of the disease. [6,7] [8]

MiRNA contribution to APP metabolism and Aβ production in Alzheimer's disease:
Identification of new miRNA-related SNPs in the 3'UTR of human APP and APOE genes

2

1.1 The multifactorial traits of Alzheimer's disease

1.1.1 Amyloid-beta peptides

The so called "senile" plaques are composed mainly of amyloid-beta (Aβ) peptides, a typically 39–43 amino acid sequence derived from the sequential proteolytic processing of the APP. [7][9] In humans, APP exists in three major isoforms that are generated by alternative splicing. APP can be processed by α-secretase in a non-amyloidogenic pathway, generating a soluble peptide designated APPα, wich only contains thea C-terminal fragment of the Aβ peptide. Alternatively, in the amyloidogenic pathway, consecutive cleavage of APP by BACE1 and the γ-secretase complex generates the soluble APPβ, Aβ peptide and the AICD which can be further cleaved by caspases (figure1). [10]
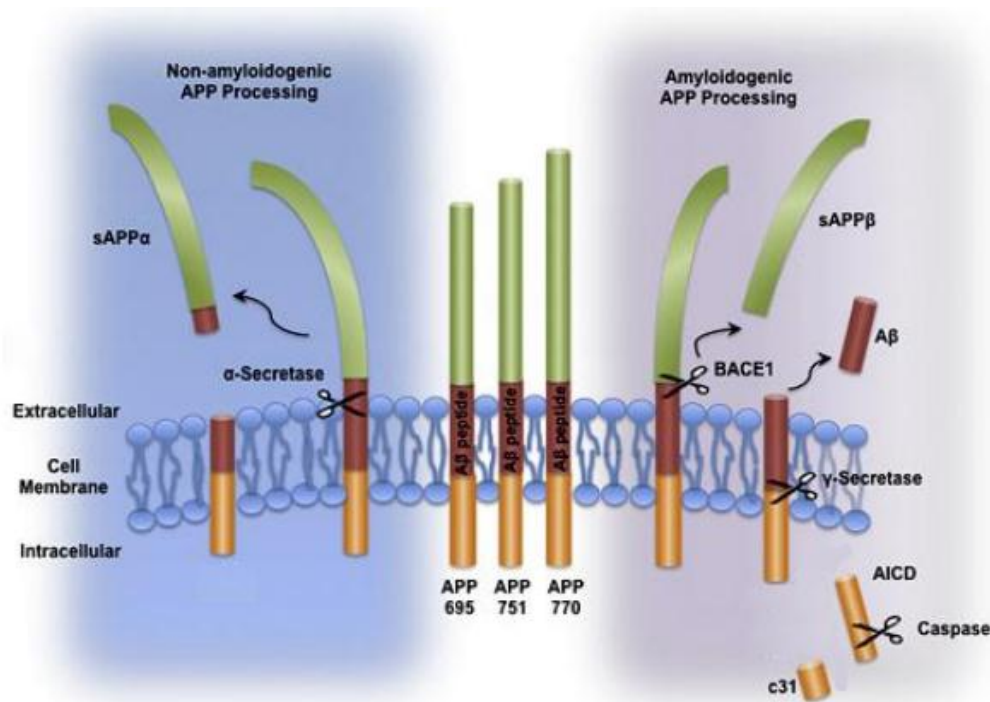
Figure 1. Schematic drawing of the Amyloid Precursor Protein (APP) and its processing pathways. In humans, APP exists in three major isoforms that are generated by alternative splicing (APP 695, App 751 and APP 770). APP can be processed by α-secretase in a non-amyloidogenic pathway, which generates soluble APPα (sAPPα). Alternatively, in the amyloidogenic pathway, cleavage by the β-secretase BACE1 generates soluble APPβ (sAPP β), which is secreted, and a C-terminal fragment that is retained in the membrane. Subsequent cleavage of the C-terminal fragment by the γ-secretase complex generates Aβ and the APP intracellular domain (AICD) which can be further cleave d by caspases to produce a c31 fragment.[10]

Aβ peptides can be detected in the cerebrospinal fluid and often are present in conditioned media from various tissue cultures and several cell lines, suggesting that they are constantly produced and secreted [7]. Since such secretion occurs in normal healthy individuals, the presence of Aβ by itself, in its soluble, unfibrillized state, is not meaningful of a pathologic condition[9,11 12].

Despite being the most famous molecular aspect of AD and having a well established presence in several amyloid systemic diseases, studies have also shown that Aβ plaque concentrations poorly correlates with the progression and severity of the symptoms in this pathology. Moreover, transgenic animals that develop widespread Aβ plaque deposition due to mutant APP overexpression, show only slight cognitive deficits [7 13].

Neurons overburdened with intracellular Aβ peptides eventually undergo synaptic and dendritic degeneration, ultimately resulting in cellular lysis.

Experimental evidence suggests that astroglial cells are able to phagocyte Aβ peptides in a process which may be ApoE dependent[4]. Once internalized, Aβ induces functional changes in astrocytes, which included spikes in the concentration of Ca^{2+} and mitochondrial depolarizaton, resulting in oxidative stress damage, as well as reversal of the glutamate uptake system which in turn results in additional glutamate release levels exacerbating neuronal damage [14 4].

However, despite the ability of astrocytes to accumulate a substantial intracellular amount of Aβ, this process eventually leads to cellular death and culminates in the release of Aβ back to the extracellular space. [15 16]

With the increasing dispersal of cellular contents, the activity of released lysosomal enzymes leads to the formation of spherical deposition of cell residues in the form of plaques, the size of which is directly proportional to the type of the cell from which they were derived [15].

In response to cellular death, both the smaller astrocytic plaques and the larger neuronal derived plaques are rapidly infiltrated by microglia and macrophages (most of which are believed to be derived from blood monocytes) [15 14].

Once at the plaque core, microglia appears to concentrate the released Aβ and promote its fibrillogenesis within tiny, tube-like invaginations in the plasma membrane [15]. The mature amyloid fibrils could represent a cellular mechanism of detoxifying potentially harmful polypeptide

MiRNA contribution to APP metabolism and Aβ production in Alzheimer's disease: Identification of new miRNA-related SNPs in the 3'UTR of human APP and APOE genes

4

chains by sequestering them into insoluble and biologically inert materials. [13]. Meanwhile, astrogliosis is also shown to prominently occur around amyloid plaques. This could be interpreted as a mechanism to prevent the amyloid plaques from establishing contact with neurons and generate a chain reaction effect from the peptide radial extracellular dispersion .[15] [14].

Recently, the amyloid intermediates have been considered to be the true responsibles for AD pathology development and they also appear to be involved in several extra cerebral amyloid diseases like the lysozyme, transthyretin and amylin amyloidosis [13].

In AD, the soluble Aβ monomers can form higher-order assemblies ranging from low-molecular weight oligomers, like dimers and trimers, to mid range-molecular weight oligomers to protofibrils and fibrils that ultimately compose the plaques [17].

Studies show that the Aβ dimmers, trimers and other higher order oligomers secreted by cultured neurons inhibit LTP and damage neuronal spines. Additional studies have also shown that Aβ dimmers, derived from human cerebrospinal fluid disrupt synaptic plasticity and inhibit hippocampal LTP *in vivo* [18].

Multiple forms of Aβ oligomers appear to exist and co-exist in the brain tissue and are able to alter neuronal and cognitive function. Each of these forms may act on different receptors, activating either specific or unspecific signaling pathways and resulting in different consequences to neuronal synaptotoxicity and survival, with different effects at different times during the evolution of the disease. [17] Therefore, blocking the initial overproduction and accumulation of Aβ in neurons can be considered a promising target from a therapeutical standpoint.

1.1.2 The neurofibrillary tangles

NFTs are composed of paired helical filaments, which are structures made of abnormal hyperphosphorylated forms of the microtubule-associated protein Tau, presents a size between 10nm and 20nm width with a half periodicity of 80 nm, and reaching an average of 300–600nm in length. [4] [19] [20]

The Tau protein is encoded by a single gene (MAPT) located on chromosome 17, although it is alternatively spliced to yield six major protein isoforms in the adult human brain. The

MiRNA contribution to APP metabolism and Aβ production in Alzheimer's disease:
Identification of new miRNA-related SNPs in the 3'UTR of human APP and APOE genes

5

alternative splicing of exon 10 yields isoforms with either three or four repeated domains, referred to as 3R and 4R Tau, depending if exon 10 is absent or present, respectively.[21]

Tauopathies can be distinguished based on the predominant tangle isoform. For instance, in AD both 3R and 4R tau accumulate in neurofibrillary tangles while in Pick's disease only marked 3R Tau can be found.[21]

The Tau fibrillization pathway is thought to consist of at least three key steps. First, the microtubule binding function of Tau is neutralized so that Tau protein can accumulate in an assembly competent form at a specific intracellular location. Second, Tau molecules must self-associate through their microtubule binding repeat regions to form the β-sheet enriched filaments observed in the brain. At last, the third step involves the nucleation of tau filament and formation of mature NFTs. Hyper phosphorylation can occur in all of these steps. [20]

High levels of NFTs block the transport of nutrients and other essential molecules throughout the cell, ultimately leading to neurite distrophism. The tangles form aggregates conjugated with ubiquitin, a property shared with other aggregating intraneuronal proteins, such as α-synuclein. [22] [7]

In AD, the lesions seem to develop in a pattern fashion, which reflects the sequence, type and severity of cognitive decline and neuronal loss. Studies suggest that Tau fibrillization can be used as a marker for the disease, correlating with both cognitive decline and neurodegeneration. In transgenic animals, the presence of Tau revealed to be significant for Aβ to exert its toxic effects, thus reinforcing the significance of NFT's in AD. [10] [20]

To better understand the role of NFTs in this condition, triple-transgenic mice, referred to as 3xTg-AD, were developed as a model for AD. This model was developed by microinjecting the APP_{swe} and Tau_{P301L} genes into single-cell embryos of $PS1_{M146V}$ KI mice. The 3xTg-AD mice progressively develop Aβ and Tau pathology with a temporal- and region-specific profile that closely mimics pathological development in the human AD brain [21].

In this model, Aβ deposition develops before the tangle pathology. Whereas extracellular amyloid deposits manifest by six months of age, conformational changes of Tau are not apparent until approximately 10-12 months of age. Tau immunostaining reveals a hierarchal pattern to the Tau staining. The first marker to appear is MC1, followed by phophospecific markers, such as AT8

MiRNA contribution to APP metabolism and Aβ production in Alzheimer's disease:
Identification of new miRNA-related SNPs in the 3'UTR of human APP and APOE genes

6

and AT180, and finally PHF-1. These results indicate that Tau undergoes conformational changes before becoming hyperphosphorylated. [21].

Again, despite being the first hallmark to arise, Aβ initial deposition was shown to be insufficient to trigger the key aspects of AD, one of them being neuronal loss, pointing NFT's as the likely responsible for the neurodegeneration and LTP deficits that occur in AD [21].

1.1.3 ApoE

ApoE is a glycoprotein synthesized as an 18 amino acid N terminal signal peptide that undergoes intracellular processing before being secreted in a 35 kDa mature form containing 299 amino acids. It contains amphipathic α-helical domains that conformationally adapt, in a reversible manner, between a lipoprotein-bound and a lipid-free state and act as a ligand for the LDL receptor [23] [24] [25].

The protein is encoded by a 3.6 kbp Gene, with 4 exons, located on chromosome 19 [24].

The physiological role of ApoE is exerted in lipoprotein particles, an assembly of both proteins and lipids that are responsible for the intracellular and extracellular trafficking of lipids. The cholesterol transport function of ApoE involves interaction with the cell surface receptor ABCA1 that promotes efflux of cellular cholesterol to the acceptor lipoproteins. ApoE also functions as a ligand in receptor-mediated endocytosis of apo E-containing lipoproteins, allowing them to bind and be internalized by receptors of the LDL receptor family wich are located on the cell surface of neurons. [24] [26] [27]

There are lipoproteins of different size classes in plasma, mainly synthetized by the liver and gut. Plasma ApoE, in particular, originates predominantly from the liver but is expressed as well in a wide variety of other tissues, including the brain, spleen, lungs, ovary and kidney[24] [28]. Exchange between liver and brain-derived ApoE and ApoE-containing lipoproteins does not take place due to the blood-brain barrier, meaning that all the brain ApoE must be synthetized locally. [29]

In the CNS, ApoE it is the most abundantly produced apolipoprotein and is predominantly expressed by astrocytes, but also microglia, in nascent high-density lipoprotein (HDL)-like particles.

MiRNA contribution to APP metabolism and Aβ production in Alzheimer's disease:
Identification of new miRNA-related SNPs in the 3'UTR of human APP and APOE genes

7

In the occurrence of excitotoxic injury, ApoE is also found to be expressed in neurons of the hippocampus and cortex [28] [26].

Cholesterol depletion, or a lack of cholesterol delivery, causes synaptic and dendritic spine degeneration and results in failed neurotransmission and decreased synaptic plasticity culminating in neuronal cell damage and eventually cellular death. On these conditions, ApoE is up-regulated for clearance and redistribution of cholesterol the lipid debris [24].

Since it has been shown that cholesterol-containing ApoE lipoproteins are required for synapse formation, in vitro, via a mechanism that is dependent upon functional ApoE receptors, which are up-regulated in regenerating peripheral nerves, it is suggested that the importance of ApoE is not limited to cholesterol homeostasis, but is also related to neuronal plasticity, neurite growth and synaptogenesis [24] [28] [26].

Humans have 3 common ApoE isoforms that result in single aminoacid substitutions trough SNPs: ApoE2, ApoE3 and ApoE4. Each one differ from the others only at the 112th and/or 158th aminoacids. For instance, ApoE3 contains a cysteine at position 112 and an arginine at 158 while ApoE2 contains cysteines at positions 112 and 158 and ApoE4 contains arginines in both sites [24] [28].

The high allelic frequency of ApoE isoform E3 in the human population and the lack of strong association of this isoform with a human disease phenotype, points ApoE3 as the human "wild-type". Curiously, ApoE4 appears to be the ancestral form, since the Arg residues at sequence positions 112 and 158 are strongly conserved across almost all animal species possessing ApoE [30] [24].

Each one of this isoforms bears distinct structural and functional properties as discriminated in Table 1 [24] [28] [23].

MiRNA contribution to APP metabolism and Aβ production in Alzheimer's disease:
Identification of new miRNA-related SNPs in the 3'UTR of human APP and APOE genes

8

Isoform	Average allelic frequency (%)	Amino acid variation (residue)		Functional differences		Structural differences		Associated disorders
		112	158	LDL receptor affinity	Lipoprotein-binding preference	Conformational stability and folding behavior	Domain interaction?	
ApoE2	7	Cys	Cys	Low	HDL	Most stable and lacks folding intermediates	No	Type III hyperlipoproteinemia
ApoE3	78	Cys	Arg	High	HDL	Intermediate stability with folding intermediates	No	Unknown
ApoE4	15	Arg	Arg	High	VLDL LDL	Least stable with folding intermediates	Yes	Alzheimer's disease and other neurological conditions; atherosclerosis

The LDL receptor binding activity of ApoE2 is approximately 1% of that of the parent isoform, while ApoE3 and ApoE4 bind to LDL receptors with similarly high affinity. As a result, ApoE2 is associated with type III hyperlipoproteinemia, a lipid disorder characterized by increased plasma levels of cholesterol and triglycerides [23].

The most pronounced pathology attributable to ApoE polymorphism in humans is the association of ApoE4 with neurodegenerative diseases, in particular with Alzheimer's disease [24].

ApoE4 is a major risk factor for AD. Those who inherit one ApoEε4 gene not only possess increased risk of developing AD but also an increased chance of pathology onset at an earlier age, in comparison to those who inherit the ε2 or ε3 forms of the ApoE gene. The risk of developing AD is proportional to the genetic amount of the ε4 allele, meaning that individuals who are homozigotic for the ApoEε4 gene have an even higher chance of developing AD [1].

The plasma concentration of ApoE in ε4 homozygous human carriers is lower than that observed in individuals possessing two ε3 alleles. Furthermore, such individuals manifest elevated plasma cholesterol and LDL levels. More importantly, the inheritance of ApoE4 is correlated with cerebral amyloid angiopathy, tauopathies and dementia, not only in AD but also in Parkinson's disease and multiple sclerosis[1] [24].

It is noteworthy that being a susceptibility gene means that its sole presence is neither necessary nor sufficient for the development of Alzheimer's disease. Moreover, the full influential aspects of ApoE haplotypes upon Aβ and tau are still to be determined [1]. There seems to exist an isoform-dependent propensity (ε 4> ε 3> ε 2) for Aβ to be deposited as cerebral amyloid plaques in experimental animals and in humans. ApoE4 carriers have also shown increased cerebral amyloid deposition in comparison with noncarriers [12] [31].

MiRNA contribution to APP metabolism and Aβ production in Alzheimer's disease:
Identification of new miRNA-related SNPs in the 3'UTR of human APP and APOE genes

9

The ApoE genotype also seems to affect the lipidation states of apolipoproteins and Aβ peptides in the cerebrospinal fluid [32].

Despite having a reportedly higher lipid binding affinity than its counterparts, the ApoE4 physiological ability to promote cholesterol efflux is remarkably lower than that of ApoE3 and ApoE2, presumably due to the structurally limited interactions of ApoE4 with ABCA1 receptors[28] **[24]**.

ApoE degradation is preferentially conducted by astrocytes, with lipidated ApoE being less susceptible to proteolysis than lipid-free ApoE. This may explain the genotype-dependent ApoE total levels in brain and CSF, when the ε4 allelle shows the lowest protein levels, followed by ε3 and with ε2 correlating with the highest protein levels **[24]**.

Since apoE4 fragments have been co-localized with amyloid deposits in plaques and also in neurofibrillary tangles in the brains of AD patients, the apoE genotype correlation in both protein levels and propensity to Aβ plaque formation may be suggestive that apoE4 digestion products contribute to amyloid plaque formation and overall AD pathology [26]. Studies have shown that Aβ and delipidated apoE4 promote fibril formation more rapidly and with higher density in comparison to other apoE isoforms. It is possible that degradation by-products of delipidated ApoE can somehow act as a catalyst in Aβ plaque formation **[24]**.

Another factor that influences the amount of Aβ deposited is the extent of lipidation of the ApoE protein. Lipid-free and lipid-bound apo E exists in different conformations and the affinity of lipidated apo E for soluble Aβ is greater than that of poorly-lipidated ApoE. [26] Lipidated ApoE seems to facilitate the cellular uptake of Aβ trough the endocytosis of a complex of ApoE-containing lipoprotein particles bound to Aβ. Furthermore, ApoE has been shown to directly enhance both the degradation of Aβ within microglial cells and the ability of astrocytes to clear diffuse Aβ deposits (figure2) [28].
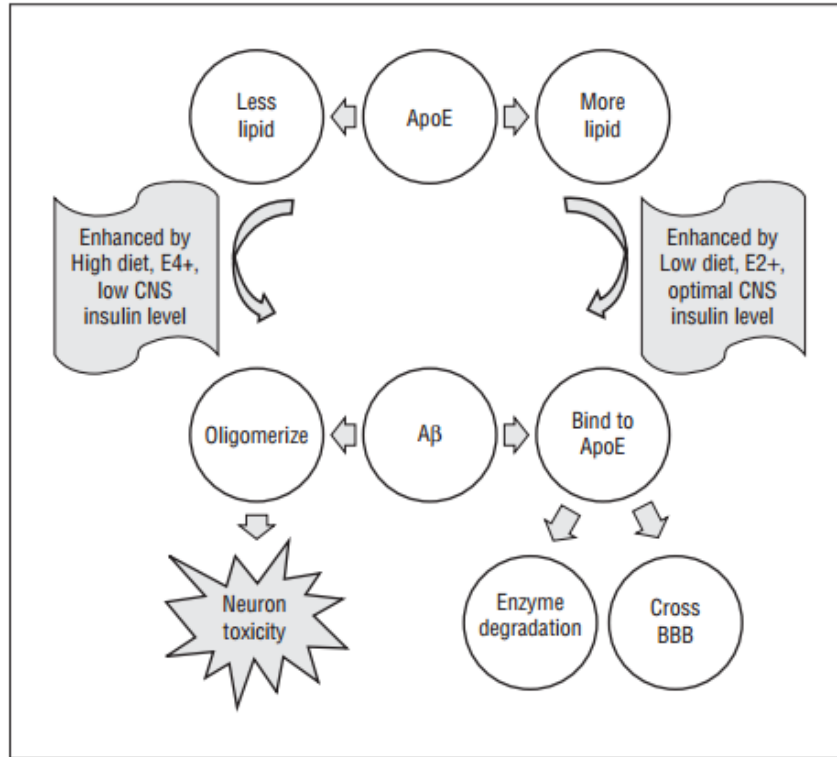
Figure 2. Schematic model of Aβ peptide and ApoE interaction in the CNS. When ApoE is more lipidated, it presents higher propensity for Aβ binding, which facilitates its clearance and degradation. When ApoE is less lipidated, which occurs when the ApoE4 isoform is present, it is less able to bind Aβ. When Aβ binds to carrier proteins, such as ApoE, it is more likely to be cleared through enzymatic degradation processes or cross the blood-brain barrier (BBB). However, when Aβ is not bound to proteins, it is more prone to oligomerization. Aβ oligomers are toxic to synapses and neurons [32].

The cellular internalization of the lipoprotein-Aβ complex is mediated by the LDL receptor family by receptor-mediated endocytosis. Therefore, since it was shown that Aβ can be internalized in the absence of ApoE, it is possible that the Aβ will undergo different endocitic routes depending on the activated internalization method [33].

Lipoprotein-Aβ complexes also contribute to Aβ removal from the brain to the systemic circulation by both endocitic and receptor-mediated transport across the blood brain barrier, allowing for both hepatic and renal Aβ systemic clearance [34].

Regarding tau, several studies of ApoE overexpression in mice were able to correlate the ApoE4 isoform with increasing levels of hyperphosphorylated tau in neurons. Since neuronal ApoE expression only seems to occur as a damage induced response, the physiological significance of these studies sugest that the ApoE influence, upon the thauopathic profile of AD, to be dependent of already established neuronal damage. [35,36] At the molecular level, ApoE interaction with LDL

MiRNA contribution to APP metabolism and Aβ production in Alzheimer's disease:
Identification of new miRNA-related SNPs in the 3'UTR of human APP and APOE genes

11

receptors was shown to inhibit several tau kinases like P35, P-GSK3β and CDK5, effectively resulting in lower tau phosphorylation levels [37].

Despite the relationship between ApoE and tau phosphorylation, human CSF tau and phosphorylated tau levels were shown to have no correlation with ApoE haplotypes, suggesting that ApoE4 may influence AD onset mainly via an Aβ related mechanisms [12 38].

Only about one percent of the AD cases are known to be caused by rare genetic mutations. These mutations can involve autosomal dominant gene mutations and/or duplications in the locus for the amyloid precursor peptide (APP) on chromosome 21, for the presenilin 1 protein on chromosome 14, and for the presenilin 2 protein on chromosome 1[4,22]. Inheriting any of these genetic mutations guarantees that an individual will develop AD in a clinically indistinguishable pattern from the sporadic form. In such individuals, the disease tends to develop before the age of 65, sometimes in individuals as young as 30. People inheriting this mutations or that possess more than one close relative already diagnosed with AD are said to have the "familial" form of AD and account for about 5% of all documented AD cases[22 39].

The remaining 95% of all cases of AD are considered sporadic forms of the disease, from which over 60% are not associated with ApoE genotype, suggesting that other genetic or maybe environmental factors may contribute to this disease onset.

Taken together, both the accumulation of insoluble protein aggregates and gene duplications verified in AD emphasize the importance of protein expression deregulation in this pathology.

1.2 MicroRNAs

MiRNAs are small non-coding RNAs that control gene expression at the posttranscriptional level. On a neurobiological context, they are essential for neuronal function and survival [40].

These short (approximately 21-23 nucleotides) conserved non-protein-coding RNAs are transcribed from the genome [40]. In mammals, more than one thousand miRNAs have been identified and approximately one-third of miRNA genes are located within introns of protein-coding messenger RNAs (mRNAs), while the remaining are intergenic. After transcription, miRNA precursors are cleaved in the cytoplasm by the RNase Dicer to produce small double-stranded

MiRNA contribution to APP metabolism and Aβ production in Alzheimer's disease:
Identification of new miRNA-related SNPs in the 3'UTR of human APP and APOE genes

12

nonprotein-coding RNAs. Successive processing of the miRNA precursor molecule generates a single-stranded miRNA (mature miRNA) [40] [41].

Mature miRNAs latter function as part of the RNA-induced silencing complex (RISC), which targets specific mRNA transcripts preferentially located in the 3'UTR of genes. Binding of the miRNA to its target leads to translation inhibition and/or mRNA degradation of the target [40] [42,43] [43] [41].

Despite having their maturation processes and regulatory functions taking place in the cytoplasm, miRNAs were also detected in the circulating plasma. Even with the high concentration of RNAses, circulating miRNAs still show significant stability since they are believed be incapsulated in lipid structures known as exossomes [44,45].

A miRNA "family" is defined as a group of miRNAs sharing the same seed region (sequence between the 2nd and 8th nucleotide of the miRNA) and that in most, but not all, cases might target the same gene [40].

It is predicted that 25 to 70% of all protein-coding genes can be regulated by miRNAs, depending on the developmental, cellular, and/or physiological context. Moreover, a single miRNA can target up to several hundred genes, thus potentially regulating multiple biological pathways, including those implicated in neuronal survival [40] [42].

This potential multiplicity of gene targeting makes assessing and proving that a specific gene or pathway is indeed a target of a particular miRNA an elusive and nontrivial task. A major disadvantage in miRNA research is the difficulty in validating putative target mRNAs predicted for a specific miRNA. There are available variety of online algorithms that utilize different approaches to predict miRNA–mRNA interactions, but the predicted targets for each miRNA in each database might be dissimilar, largely non-overlapping and often exclude many experimentally proven and validated targets [46].

1.2.1 MiRNAs in Alzheimer's disease.

Results from recent profiling experiments in humans suggest that a number of specific miRNAs are misregulated in disease conditions, several of which have been implicated in the regulation of key genes involved in AD, including APP, BACE1 and MAPT. Moreover, rare disease-specific polymorphisms have been identified in known and putative miRNA target sites of APP and BACE1 genes [40].

Several miRNAs are expressed specifically in neurons, where some are proposed to function in neuronal activities, such as neurite outgrowth and synapse formation. In fact, there are some interesting parallels that can be established between a Dicer-deficient brain and an AD brain. A Dicer-deficient brain lacks functional miRNAs due to the absence of the Dicer enzyme, which cleaves miRNA's precursors into single-stranded functional miRNAs (mature miRNAS). Neuronal Dicer cKO mice develop progressive neurodegeneration, presenting reduced brain size, enlarged ventricles, neuroinflammation, apoptosis (in some cases), as well as impaired dendritic branching and spine length. In addition, neuronal Dicer cKO mice exhibit AD-like hyperphosphorylation of endogenous Tau, which is not observed in non-transgenic mice. Such results further reinforce the idea of AD as a miRNA dysfunctional disease [41,47].

Specific loss of Dicer in oligodendrocytes results in axonal degeneration accompanied by abnormal axonal transport and endogenous APP accumulation. This model also displays signs of oxidative stress, and, taken together, these results point out the importance of Dicer and miRNAs in maintaining neuronal function [47].

The impact of miRNA modulation of APP metabolism and Aβ production seems to be intimately involved and of major relevance in AD development (Figure 3). Therefore, aspects inherent to AD that compromise miRNA function may not be only restricted to variations in miRNA levels [42].

MiRNA contribution to APP metabolism and Aβ production in Alzheimer's disease:
Identification of new miRNA-related SNPs in the 3'UTR of human APP and APOE genes

14
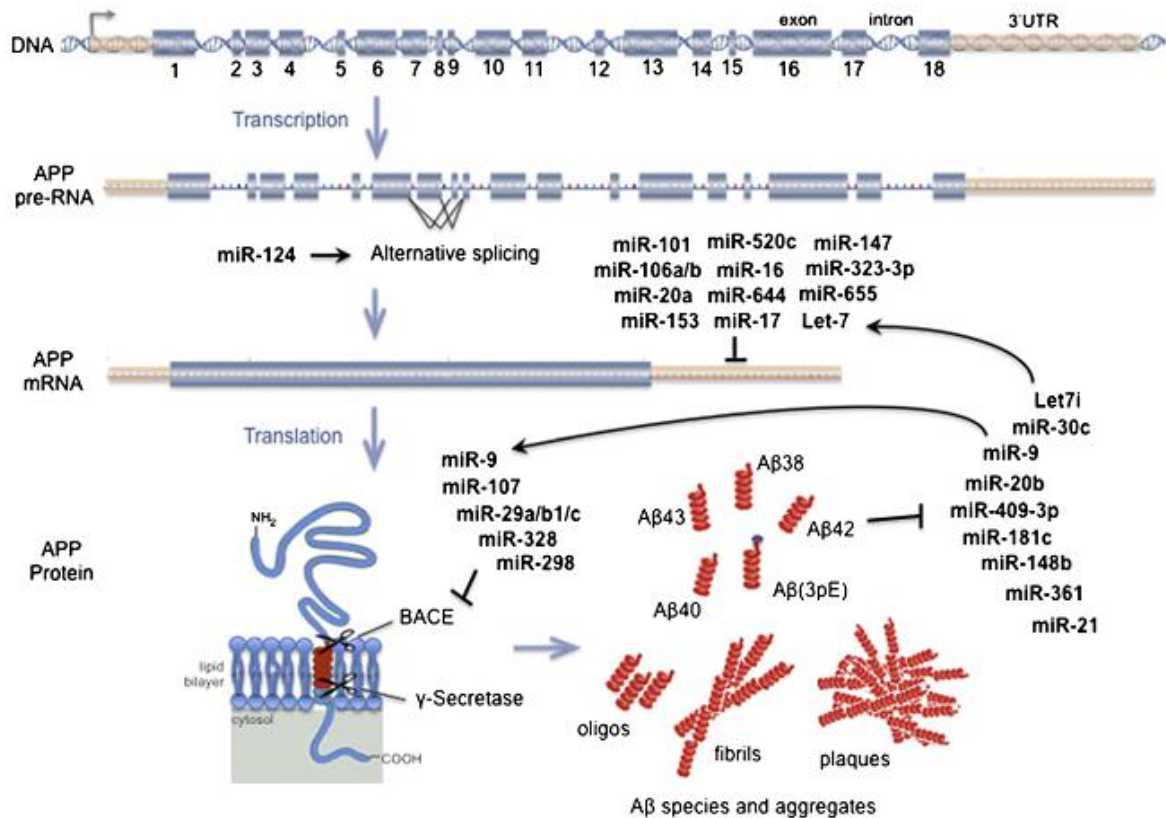
Figure 3. Schematic representation of the miRNA network surrounding APP. Both upstream and downstream components directly or indirectly affect APP processing and Aβ metabolism [42].

The hypothesis of a secondary factor, besides miRNA transcription levels influencing miRNA, lies in AD-specific genetic mutations in the 3'UTRs of APP, BACE1 and ApoE genes, which can either abolish existing miRNA binding sites or create new illegitimate miRNA binding sites that could contribute significantly an increased risk of developing this neurodegenerative disorder. [42].

1.2.2 3'UTR SNPs and their effects on miRNA function in AD

The known AD specific APP variants that arise from such mutations are T171C, A454G and A833C (figure 4) [42].

When assessing the effects of miRNAs in the regulation of the several variants of APP, it was observed that MiRNA-147 was significantly affected by the T171C mutation when compared to the wild-type construct, showing a propension to inhibit APP expression in the presence of the T171C SNP. On the other hand, miRNA-20a, but not miRNA-17, was affected by the A454G mutation, further decreasing the expression of APP in the presence of A454G SNP [42].
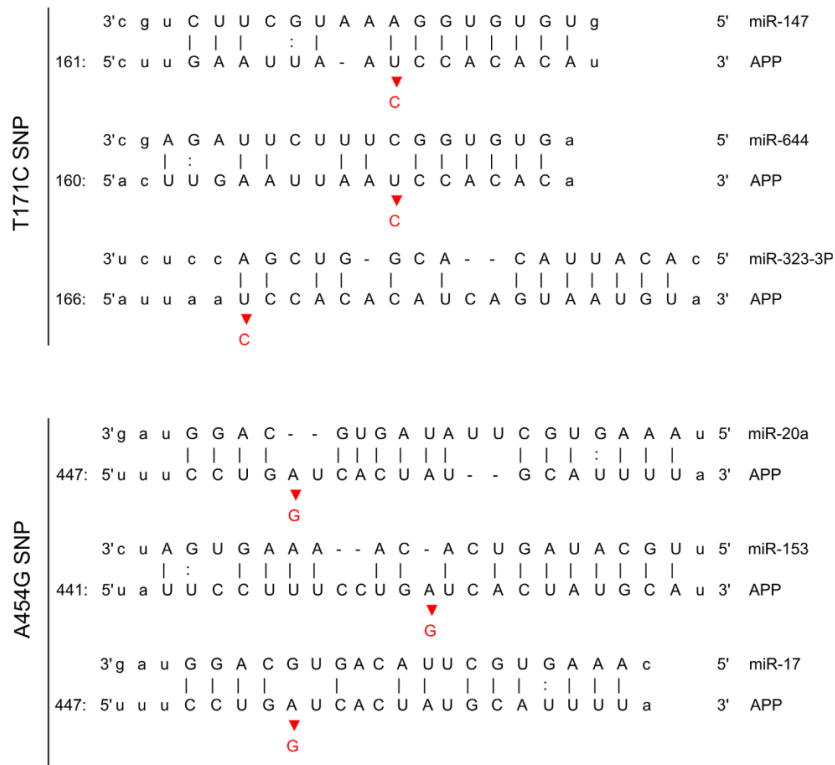
Figure 4. **Schematic representation of base pair matching between miRNAs and the 3'UTR of human APP. The seed region of the miRNAs is indicated. The red bases represents the SNPs T171C (upper panel) or A454G (lower panel). Adapted from [42].**

For miRNA-147, the effect may be explained by the fact that T171C is located immediately adjacent to the miR-147 seed region binding site, therefore directly inhibiting miRNA binding. This effect can also be theoretically explained by the increase in the required binding energy between miR-147 and the 3'UTR of APP, which makes the binding less favourable, therefore decreasing the ability of this miRNA to modulate APP levels [42].

MiRNA contribution to APP metabolism and Aβ production in Alzheimer's disease:
Identification of new miRNA-related SNPs in the 3'UTR of human APP and APOE genes

16

Such results show that polymorphisms located in the 3 'UTR region of APP may affect the expression of this protein. More importantly, these polymorphisms may constitute a new aspect to consider when developing new diagnostic tools and miRNA dependant therapies[42].

Aiming at better comprehending the genetic features of AD pathogenesis that contribute to miRNA dysfunction, in the context of this disease, we propose a two way approach, based on the identification of unknown SNPs in the 3'UTR of the APP and APOE genes of both AD patients and healthy controls and on the evaluation of the ability of specific miRNAs to modulate APP production in neuronal cells.

MiRNA contribution to APP metabolism and Aβ production in Alzheimer's disease:
Identification of new miRNA-related SNPs in the 3'UTR of human APP and APOE genes

17

Objectives

2. Objectives

This study aims to establish a SNP profile of the 3'UTR of APP and ApoE genes, in AD patients, in order to evaluate their significance as modifiers of miRNA function and their contribution to AD onset and severity.

The specific goals of the study are:

- To identify SNPs in the 3'UTRs of the APP and ApoE genes, and evaluate the significance of this SNPs as modifiers of miRNA function and AD development;
- To perform a validation study on the miRNA binding strength and APP modulation capacity of miRNAs predicted to target the 3'UTR of the human APP gene, aiming at identifying miRNAs capable of decreasing APP production in a therapeutic setting.

MiRNA contribution to APP metabolism and Aβ production in Alzheimer's disease:
Identification of new miRNA-related SNPs in the 3'UTR of human APP and APOE genes

19

Materials and Methods

MiRNA contribution to APP metabolism and Aβ production in Alzheimer's disease:
Identification of new miRNA-related SNPs in the 3'UTR of human APP and APOE genes

20

3. Materials and Methods

3.1 Materials

NZY Blood gDNA isolation kit, NZYgelpure PCR purification kit,NZYTaq DNA polymerase, dNTPs, and $MgCl_2$ were purchased from NZYtech (NZYtech, Portugal). The custom designed primers were obtained from Alfagene (Alfagene, Portugal) GenomeLab™ DTCS Quick Start Kit was obtained from IZASA. Plasmids for miRNA-485-5p and APP 3'UTR reporter expression were purchased from OriGene. The Lipofectamine™ LX Transfection Reagent was purchased from Invitrogen.

3.2 Subject selection and sampling

All participants in this study were recruited at the Dementia Clinic from the University of Coimbra Hospital Center and were subjected to a detailed clinical and psychiatric examination.

According to their clinical status, the subjects were divided into 3 groups: healthy controls (group 1, n=12), AD patients (group 3, n=25) and patients with MCI (group 2, n=18). For the establishment of the control groups only individuals with no prior history of neurological or psychiatric diseases were selected.

In individuals diagnosed with AD or MCI, the diagnose was further confirmed through imaging studies, measurement of hippocampus atrophy, ApoE genotyping and AD biomarker profiling, including quantification of Aβ42, total tau and phosphorylated tau levels in the cerebrospinal fluid.

A 20 mL blood sample was collected from each subject into sterile EDTA coated tubes, according to a protocol approved by the ethics committee of the hospital and after receiving a written consent from the study participants or their next of kin.

MiRNA contribution to APP metabolism and Aβ production in Alzheimer's disease:
Identification of new miRNA-related SNPs in the 3'UTR of human APP and APOE genes

21

3.3 DNA storage and extraction from blood samples

From each 20 mL sample, 200 μL of blood were withdrawn for storage into genomic DNA cards (Nucleocard, Macherey-Nagel) and 400 μL were separated for DNA extraction.

DNA extraction was performed using the NZY Blood gDNA isolation kit. Briefly, 225 μL of a proteinase K-containing lysis buffer was added to a 200μL blood sample, vortexed and incubated for 15 minutes at 56°C. In order to provide proper DNA binding conditions to the silica-based purification columns, a volume of 210 μL of ethanol was added to the sample, followed by homogenization trough vortex. The resulting solution was applied into the purification columns and underwent a short centrifugation of 1 minute at 11.000 g. Two follow-up centrifugations with washing buffers NW1 and NW2, also performed at 11.000 g during 1 minute, minimized the non-specific interactions of other molecules with the purification column.

Finally, after drying the column through a 2 minutes long 11.000 g centrifugation, the purified DNA was eluted by incubating the column with 50μL of sterile water for 1 minute followed by another centrifugation of 2 minutes at 11.000 g.

The purified DNA samples were quantified using a NanoDrop device and stored at -20°C. The purity of the samples was evaluated taking into consideration their 260nm/280 nm and 260/230 nm ratios.

3.4 Primer design

NCBI's primer blast tool combines the primer designing capabilities of the Primer3 software with BLAST and global alignment algorithms, allowing the custom design of PCR primers according to any available nucleotide sequence databases.

The 3'UTR sequences of both APP and APOE were obtained through the Ensembl (ensembl.org) and MiRNA.org (miRNA.org) databases and cross-referenced with GRCh37.p10 genomic build trough NCBI (ncbi.nlm.nih.gov).
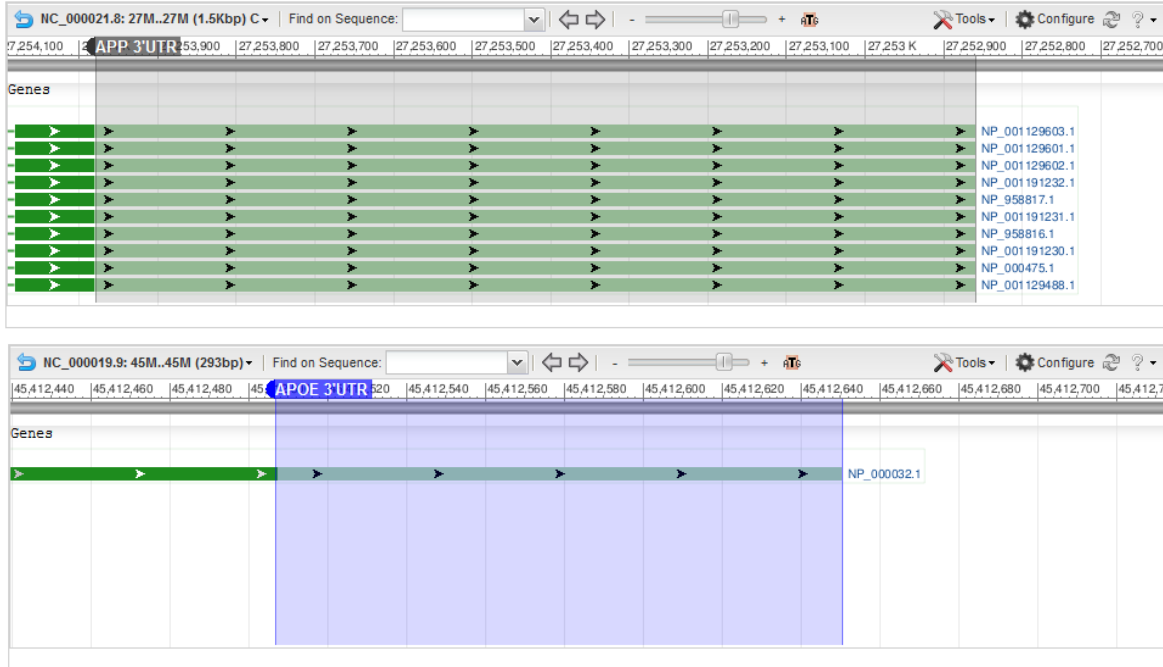
MiRNA contribution to APP metabolism and Aβ production in Alzheimer's disease:
Identification of new miRNA-related SNPs in the 3'UTR of human APP and APOE genes

22

Figure 5. NCBI interface of the 3'UTR regions of both the APP and ApoE genes and neighboring sequences. The APP 3'UTR is highlighted in black and the ApoE 3'UTR is highlighted in blue. Each of the green bars in the APP gene is representative of a distinct APP isoform.

Primer locations were aimed at the 3' and 5' flanking sequences of the desired templates in order to comprise the entirety of the 3'UTR sequence upon amplification and sequencing.

Due to the extent of the APP's 3'UTR sequence (1119 bp), two additional primers were designed in order to decrease possible sequencing errors. As such, the APP 3 UTR was sequenced and analyzed through 4 contiguous sequences.

Only primers that didn't exhibited any predictable dimerization or hairpin structures were considered viable for optimization. The prediction of secondary structures was performed trough OlogoCalc (basic.northwestern.edu/biotools/OligoCalc)

MiRNA contribution to APP metabolism and Aβ production in Alzheimer's disease:
Identification of new miRNA-related SNPs in the 3'UTR of human APP and APOE genes

23

3.5 APP and ApoE 3'UTR DNA amplification

The 3'UTRs of both the APP and ApoE genes were amplified from the DNA isolated from the blood of each study participant using PCR.

A standard master mix template (table 2) and custom PCR conditions, using a gradient of annealing temperatures, were used to optimize the specificity of the designed primers and final product yield.

For each reaction, 22,5 µL of Master Mix were added to 2,5 µL of DNA at a 10 ng/µL concentration.

Table 2.Standard master mix template used in the PCRs

Master mix	Stock	Desired concentration	reaction volume
Reaction buffer	10 x	-	2,5 µL
dNTP mix	5 mM	200 µM	1 µL
Primer FW	10 µM	0,5 µM	1,25 µL
Primer RE	10 µM	0,5 µM	1,25 µL
NZYTaq	5 U/µl	0,04 U/µl	0,2 µL
MgCl2	50 mM	1,5 mM	0,75 µL
Nuclease-free water			15,55 µL

The amplification conditions used for each 3'UTR are discriminated in Tables 3 and 4

Table 3. Amplification conditions used for the amplification of the 3'UTR of APP.

APP			
Cycle step	temperature	time	cycles
Initial denaturation	98°C	1min	1
Denaturation	98°C	10s	35
Annealing	61°C	10s	
Extension	78°C	1min 20s	
Final extension	78°C	5min	1
Storage	4°C	*ad infinitum*	

MiRNA contribution to APP metabolism and Aβ production in Alzheimer's disease:
Identification of new miRNA-related SNPs in the 3'UTR of human APP and APOE genes

24

Table 4. Amplification conditions used for the amplification of the 3'UTR of ApoE.

ApoE			
Cycle step	temperature	time	cycles
Initial denaturation	98°C	1min	1
Denaturation	98°C	10s	35
Annealing	59°C	10s	
Extension	78°C	20s	
Final extension	78°C	5min	1
Storage	4°C	*ad infinitum*	

The resulting PCR products were confirmed by agarose gel electrophoresis, using a 1,5% weight/weight agarose gel stained with greensafe. A reaction tube containing 25µL of Master Mix alone was processed alongside each sample batch to act as negative control. NZYtech's NZY ladder III was used as molecular weight marker for relative comparison in all agarose gels. The resulting bands were visualized by exposing the agarose gel to UV light.

3.6 Purification of PCR Products

The PCR reactions were purified using the NZY Gelpure kit (NZYTech)

One hundred microliters of Binding Buffer were added to each PCR product and the resulting volume was transferred to a purification column. The Binding Buffer contains guanidine tiocianate, Tris-HCl and ethanol which allow DNA binding to the silica-based column. A 1 minute centrifugation at 14.000 rpm was performed, followed by the addition of 600 µL of wash solution, to remove salts, dNTPs and enzymes, and 2 consecutive 1 minute, 14.000 rpm centrifugations.

After changing the column to a new 1,5ml eppendorf, the DNA was eluted by adding 50µL of Elution Buffer (10mM Tris-HCl, pH 8,5) and performing a final 14.000 rpm centrifugation during 1 minute.

MiRNA contribution to APP metabolism and Aβ production in Alzheimer's disease: Identification of new miRNA-related SNPs in the 3'UTR of human APP and APOE genes

25

3.7 Sequencing Reaction

The sequencing reactions were performed with the GenomeLab^{TM} Dye Terminator Cycle Sequencing using the Quick Start kit, based on the Sanger method. The technique is based on the incorporation of fluorescently-labeled NTPs during the DNA chain synthesis, by a DNA polymerase. Each type of ddNTPs contains a different fluorochrome and during the sequencing reaction the labeled ddNTPs are incorporated in the 3' end of the forming DNA strand, leading to the termination of the strand's elongation due to the lack of a 3'-OH functional group. Therefore, the end result is a group of variable sized DNA sequences, each one terminating in a distinguishable fluorescent nucleotide. Briefly, each reaction tube consisted in 3 µL of DTCS Quick Start Master Mix, 1 µL of the desired primer (10 pmol/µL), 2 µL of purified PCR product (this volume could vary to a range of 0,5 µL – 10 µL depending on the PCR product's relative concentration) adjusting up to a final total volume of 20 µL with dH$_2$O.

The sequencing program consisted in 30 cycles, with each cycle presenting 3 steps, followed by holding at 4°C. The first step was a denaturation step at 90°C for 20 seconds, in order to split the DNA double helix into single nucleotide chains, followed by the annealing step at 50°C during 20 seconds and finally a 4 minute extension step at 60°C. Resulting products were stored at -20°C or immediately purified.

3.8 Purification of Sequencing Products

A mixture of 62,5µL of ethanol 95%, 3µL of NaOAc pH 4,6 and 14,5 µL of ddH$_2$O was added to each sample on a 96-well PCR plate. The plate was then sealed with Parafilm and stored at 20°C for 10 minutes.

Three consecutive centrifugations were then performed at 5.700rpm and 4°C, during 30, 10 and 5 minutes, respectively. Between each of the centrifugations, the supernatant was discarded and 200 µl of cold EtOh 70% (-20°C) were added to each well.

The sample plate was then inverted over adsorbent paper and underwent one final 10 second pulse at 700rpm to remove any remaining ethanol.

MiRNA contribution to APP metabolism and Aβ production in Alzheimer's disease:
Identification of new miRNA-related SNPs in the 3'UTR of human APP and APOE genes

26

The pellets were then ressuspended on 25μL of formamide by vortex. In order to minimize evaporation a drop of mineral oil was added before loading the samples on the sequencer.

3.9 3'UTR sequence reading and bioinformatic alignment of the sequencing products

The sequence reading was performed on a Beckman Coulter's CEQ 8000 Genetic Analysis System automatic sequencer. Briefly, the labeled DNA fragments underwent denaturation and were separated by capillary electrophoresis. Base calling was achieved by laser-induced fluorescence in four spectral channels, each one targeting a respective ddNTP fluorochrome.

All the produced sequence read files were exported as a chromatogram and further analyzed on the SEQUENCHER[tm] software from Gene Codes Corporation.

The control group sequencing reads were directly compared with the APP and ApoE 3'UTR sequences, present in the NCBI and ENSEMBLE databases, and were further used as reference sequences for direct comparison with the AD and MCI study group's sequences.

Whenever an occurrence of two overlapping peaks was identified on the chromatogram of the sequencing product, new PCR and sequencing reactions were performed in order to confirm and validate the result as a heterozygous SNP.

SNPs were evaluated to detect the deletion of predicted miRNA binding sites or the appearance of new ones using information collected from the miRNA.org, miRwalk and Diana-microT databases

MiRNA contribution to APP metabolism and Aβ production in Alzheimer's disease:
Identification of new miRNA-related SNPs in the 3'UTR of human APP and APOE genes

27

3.10 Plasmid constructs

The miRNA-485-5p expression plasmid contains the pre-miRNA nucleotide sequence with a 300 nts up- and down-stream flaking sequence (to ensure proper miRNA expression and maturation) cloned into a pCMV-MIR Vector via SgfI and MluI restriction sites.
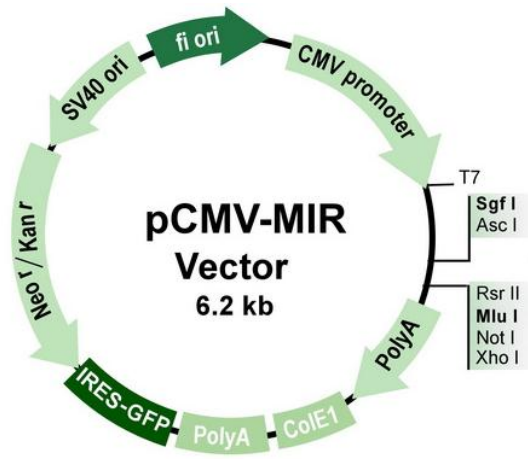

Figure 6. pCMV-MIR vertor map

The APP 3'UTR reporter clone consists in a firefly luciferase expressing vector with the APP 3'UTR sequence inserted into the plasmid after the stop codon of the luciferase. The transcript level can be therefore regulated by its interaction with miRNAs.
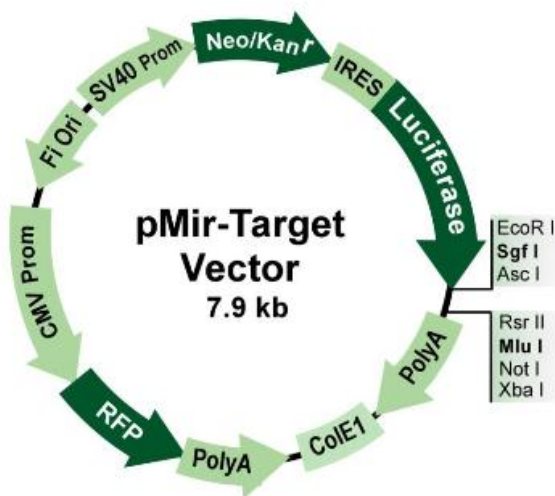

Figure 7. pMir-Target vector map

3.11 Plasmid DNA amplification

For plasmid amplification, a diluted stock of each plasmid was prepared at a concentration of 2,5 ng/μL.

The transformation of competent *E.Coli* cells was performed through a heat-shock protocol. Briefly, 2 μL of the diluted stock of each plasmid were added to 50 μL of bacterial suspension and kept on ice for 20 minutes, followed by a 30 second immersion on a 42°C bath and a second step of 2 minutes in ice.

After the transformation procedure, the bacteria were ressuspended in 350 μL of SOC medium and left incubating for 1 hour at 37°C and 220 rpm.

After incubation, 100 μL of transformed bacteria were plated on LB-Agar plates with Kanamycin (25μg/mL) and left incubating at 37°C for 16 hours.

For each plasmid, 3 individualized bacterial colonies were selected and inoculated separately in 8ml of LB-Kanamycin (25μg/mL), before undergoing a 16 hour long growth at 37°C and 220rpm.

A second 16 hour long growth at 37°C, was performed after separately transferring 1,5ml from each previous inoculation into 650 ml of LB-Kanamycin (25μg/mL), this time at 180 rpm.

3.12 Plasmid DNA purification

Plasmid purification was performed using the Nucleobond® Xtra Maxi Plus kit (Macherey-Nagel) and following the guidelines of the manufacturer.

The transformed bacteria were initially harvested by centrifugation at 6.000 g for 10 minutes at 4°C.

The pellet was ressuspended in 24 mL of ressuspension buffer, containing RNase A, before adding 24 mL of lysis buffer. The mixture was gently homogenized and left at room temperature for 5 minutes. A volume of 24 ml of Neutralization buffer was then added, followed by a 10 minute centrifugation at 5000 g.

MiRNA contribution to APP metabolism and Aβ production in Alzheimer's disease:
Identification of new miRNA-related SNPs in the 3'UTR of human APP and APOE genes

29

Meanwhile, the purification column was prepared by adding 25 ml of equilibration buffer. Once the column emptied, the supernatant was loaded, followed by the addition of 15 mL of equilibration buffer.

The column filter was then removed and washed. Elution was performed by adding 15mL of Elution buffer.

Desalting of the plasmid solution was performed by precipitating the resulting sample with 0,7 volumes of room temperature isopropanol and loading it onto a NucleoBond® Finalizer membrane by means of a syringe. After a washing step with ethanol and drying of the membrane, the pure DNA was eluted with 800μ of TRIS Buffer.

3.13 Cell culture and transfection

HEK293T cells were thawed in a 37°C water bath, transferred to a 15 mL falcon tube containing 10mL of DMEM and centrifuged at 500g for 5 minutes. After removing the supernatant, the cells were ressuspended in 20mL of DMEM and transferred to a 75 cm^2 cell culture flask.

Cells were maintained at a maximum of 90% confluence at 37°C, in a 5% CO_2 atmosphere. Cell dilution was performed by removing the growth medium, washing with 3 mL of PBS and then adding 2 mL of dissociation medium. After cell detachment, 6 mL of DMEM were added to the flask, before transferring the cell suspention to a 15 mL falcon tube (when unattended for longer than 48 hours 10 mL of DMEM were used instead to further dilute the cell suspension).

For each new flask, 1mL of the cell suspension was plated and 19 mL of DMEM were added, proceeding with another incubation period at 37°C and 5% CO_2.

For the miRNA validation experiments, the cells were detached, as previously described, counted and plated on 24-well multiwell plates at a density of 1.200.000 cells/well in a final volume of 500uL. The cells were maintained in these conditions for 24 hours until the beginning of the transfection procedure. Before transfection, cells were washed and the medium was replaced with 300μl of Optimem.

Lipoplexes were prepared by combining, the miRNA-485-5p expression plasmid and the APP 3'UTR reporter clone plasmid with the Lipofectamine™ LX Transfection Reagent for 30 min at room

MiRNA contribution to APP metabolism and Aβ production in Alzheimer's disease:
Identification of new miRNA-related SNPs in the 3'UTR of human APP and APOE genes

30

temperature in OPTIMEM. In parallel, control lipoplexes were prepared by combining the APP 3'UTR reporter clone plasmid with a GFP expressing plasmid and the same transfection reagent.

The different lipoplex formulations were then added to the plated cells aiming at a concentration of 1µg of each plasmid/well in a final volume of 500 µL.

After 4 hours of incubation, the cells were washed and the transfection medium was replaced with DMEM. Cells were then further incubated for 48 hours. At this point, the growth medium was replaced by the luciferase lysis buffer and the plates were stored at -80°C until the luciferase activity could be quantified in each sample.

3.14 Luciferase assay

The cells were thawed in ice and gently scraped from the plate. The content of each well was transferred to a separate eppendorf and centrifuged at 14000 rpm for 5 minutes at 4°C.

Fifty microliters of each supernatant were transferred to an opaque 96 well white plate.

The bioluminescent reaction was performed and luciferase activity was measured in a luminometer. Briefly, 100 µL of reading solution (containing ATP) and 100 µL of luciferin (pH 8) were added to each well in a 5 second injection. The plate was then shacked for 1 second and the luminescence levels were recorded during a 10 second interval. The luminescence values were expressed as counts per second (CPS).

Results

MiRNA contribution to APP metabolism and Aβ production in Alzheimer's disease:
Identification of new miRNA-related SNPs in the 3'UTR of human APP and APOE genes

32

4. Results

4.1 Primer optimization and 3'UTR amplification trough PCR

4.1.1 APP 3'UTR amplification

The parameters used in NCBI's primer blast search tool for the App 3'UTR amplification resulted in 3 primer pairs.

One of the selected primer pairs was designed to allow the full amplification of the APP 3'UTR, and was designated as Primer pair 1, consisting in the primers Fw1 and Re1. The other two primer pairs (Primer pair 2 and Primer pair 3) were designated to amplify smaller, but contiguous sequences of the 3'UTR.

APP 3'UTR Primer pair 1 - Fw 1 + Re 1

	Sequence (5'->3')	Template strand	Length	Start	Stop	Tm	GC%
Forward primer	CCTGTCCAAGATGCAGCAGA	Plus	20	289397	289416	60.04	55.00
Reverse primer	GGGTACCCAACATGCGAAGA	Minus	20	290677	290658	60.04	55.00
Product length	1281						

APP 3'UTR Primer pair 2 - Fw 1 + Re 2

	Sequence (5'->3')	Template strand	Length	Start	Stop	Tm	GC%
Forward primer	CCTGTCCAAGATGCAGCAGA	Plus	20	289397	289416	60.04	55.00
Reverse primer	CGCCCCGTAAAAGTGCTTAC	Minus	20	290191	290172	59.55	55.00
Product length	795						

APP 3'UTR Primer pair 3 - Fw 2 + Re 1

	Sequence (5'->3')	Template strand	Length	Start	Stop	Tm	GC%
Forward primer	GTGGGAGTTCAGCTGCTTCT	Plus	20	289877	289896	59.96	55.00
Reverse primer	GGGTACCCAACATGCGAAGA	Minus	20	290677	290658	60.04	55.00
Product length	801						

Figure 8. Primer sequences used in the amplification and sequencing of the 3'UTR of the APP gene.

Optimization of the amplification conditions was performed through several PCRs with annealing temperatures ranging from 49°C to 67°C and using a purified DNA sample from one of the control subjects. It was possible to observe that specific sequence amplification occurred for the primer pair 3 across all temperatures, although with a rather inconsistent yield, and for primer pair 2 up to 63°C.
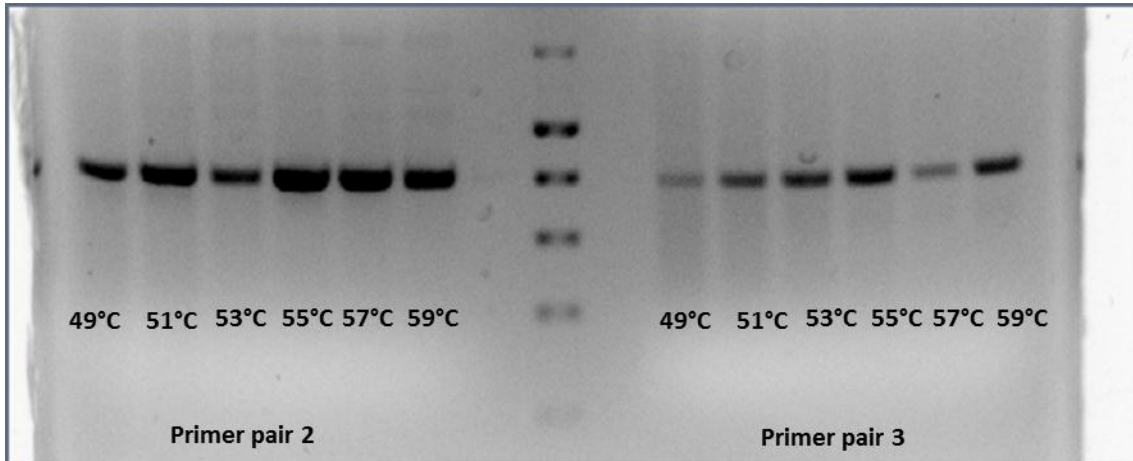
Figure 9. Representative image of the resulting bands obtained from the optimization of the APP primer pair 2 and APP primer pair 3 at the different annealing temperatures.
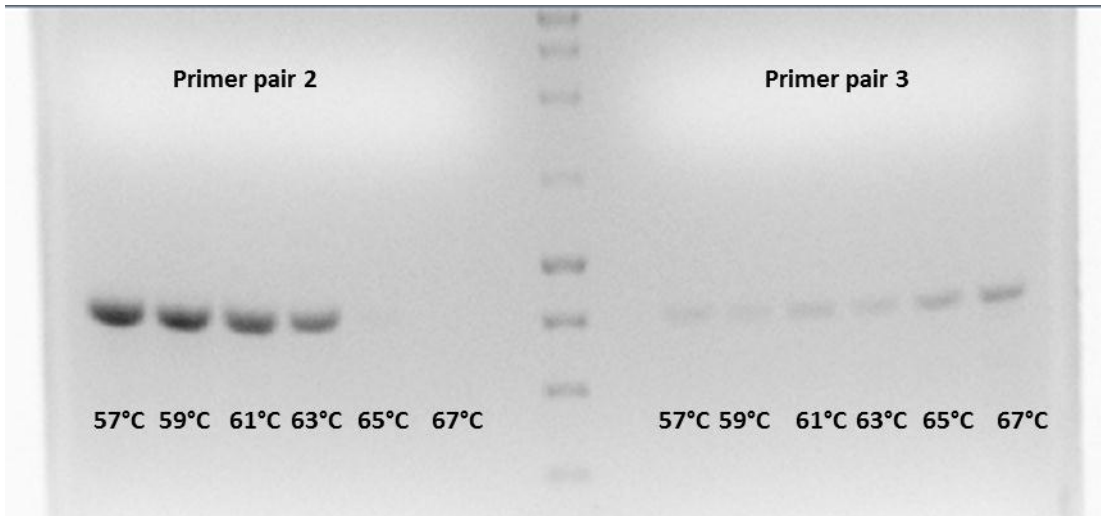

Figure 10. Representative image of the resulting bands obtained from the optimization of the APP primer pair 2 and APP primer pair 3 at the different annealing temperatures.

The ideal conditions for the complete App 3'UTR amplification were also tested trough annealing temperature gradient. The PCR was performed using Primer pair 1 in a temperature range from 57°C to 61°C and using DNA samples from 4 study subjects, in order to assess any subject related influence on the final reaction yield and primer specificity .

MiRNA contribution to APP metabolism and Aβ production in Alzheimer's disease:
Identification of new miRNA-related SNPs in the 3'UTR of human APP and APOE genes
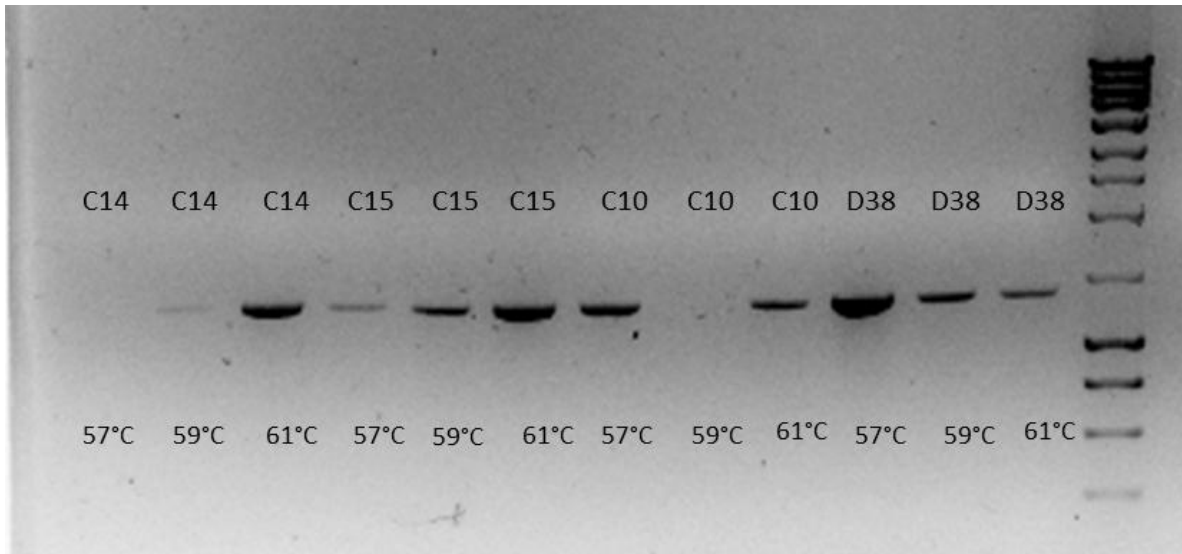
34

Figure 11. Representative image of the resulting bands obtained from the optimization of the APP primer pair 1 product in different patient samples at annealing temperatures of 57˚C, 59˚C and 61˚C.

No amplification could be observed at 57°C in subject C14 and at 59°C in subject C10. All the other condition resulted in a single band. Taken these results in consideration, all subsequent 3'UTR amplifications were performed with at 61°C annealing temperature using primer pair 1 and exhibited product specificity with similar yield.
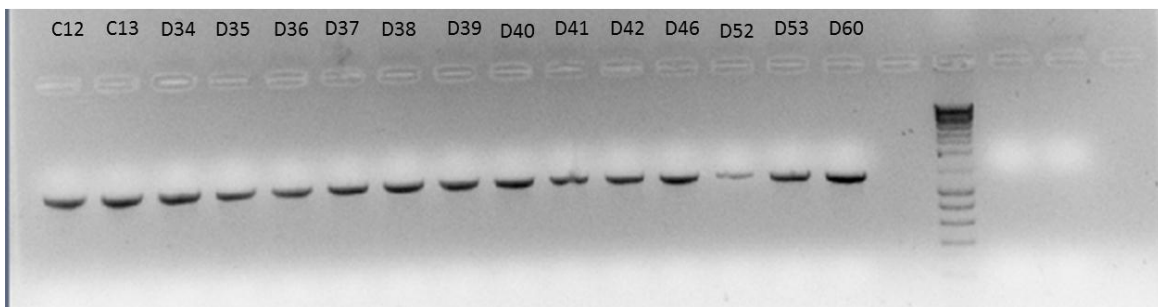

Figure 12. Representative image of the resulting bands obtained from amplification of the 3'UTR of the APP gene in 15 different samples. The bands result from the PCR products obtained by using APP primer pair 1 and an annealing temperature of 61°C.

MiRNA contribution to APP metabolism and Aβ production in Alzheimer's disease: Identification of new miRNA-related SNPs in the 3'UTR of human APP and APOE genes

35

4.1.2 ApoE 3'UTR amplification

In what concerns ApoE amplification, NCBI's primer blast search provided 4 primer pairs. The PCR conditions for amplification were optimized for each primer using a single sample and a temperature gradient in the annealing step. The temperature gradient ranged from 57°C to 61°C in intervals of 2°C.

ApoE 3'UTR Primer pair 1 – Fw1 + Re1

	Sequence (5'->3')	Template strand	Length	Start	Stop	Tm	GC%
Forward primer	CTGGTGGAGAAGGTGCAGG	Plus	19	45412442	45412460	60.00	63.16
Reverse primer	TTGTGTGGCCAGTATGTGGG	Minus	20	45412726	45412707	60.25	55.00
Product length	285						

ApoE 3'UTR Primer pair 2 – Fw2 + Re2

	Sequence (5'->3')	Template strand	Length	Start	Stop	Tm	GC%
Forward primer	GCTGGTGGAGAAGGTGCAG	Plus	19	45412441	45412459	60.67	63.16
Reverse primer	GGCCAGTATGTGGGCAGAAA	Minus	20	45412720	45412701	60.32	55.00
Product length	280						

ApoE 3'UTR Primer pair 3 – Fw3 + Re3

	Sequence (5'->3')	Template strand	Length	Start	Stop	Tm	GC%
Forward primer	GGGCTGGTGGAGAAGGTG	Plus	18	45412439	45412456	59.65	66.67
Reverse primer	GAAACTGAGGCTGGGGCTTA	Minus	20	45412698	45412679	59.67	55.00
Product length	260						

ApoE 3'UTR Primer pair 4 – Fw4 + Re4

	Sequence (5'->3')	Template strand	Length	Start	Stop	Tm	GC%
Forward primer	CAGCGACAATCACTGAACGC	Plus	20	45412492	45412511	60.18	55.00
Reverse primer	GGCCAGTATGTGGGCAGAAA	Minus	20	45412720	45412701	60.32	55.00
Product length	229						

Figure 13. Primer sequences tested in the amplification and sequencing of the 3'UTR of the ApoE gene.

The resulting PCR products were analysed trough agarose gel electrophoresis. No amplification could be observed using primer pair 1,2 and 4. Primer pair 3 exhibited specific amplification across the entire temperature range, providing the highest yield at 59°C and was, therefore, selected to perform ApoE 3'UTR PCR reactions at this annealing temperature for a set of 13 samples.

MiRNA contribution to APP metabolism and Aβ production in Alzheimer's disease:
Identification of new miRNA-related SNPs in the 3'UTR of human APP and APOE genes
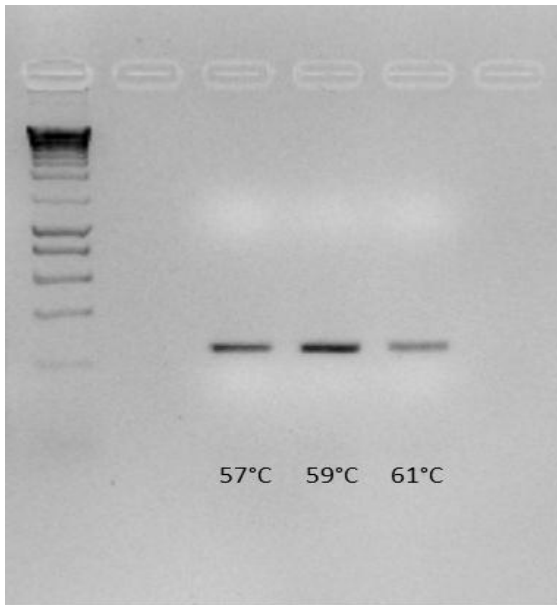
36

Figure 14. Representative image of the resulting bands obtained from the optimization of ApoE primer pair 3 at annealing temperatures of 57°C, 59°C and 61°C

In this experiment, nonspecific amplification was detected in some samples by the presence of an unexpected band with approximately 700 bp.
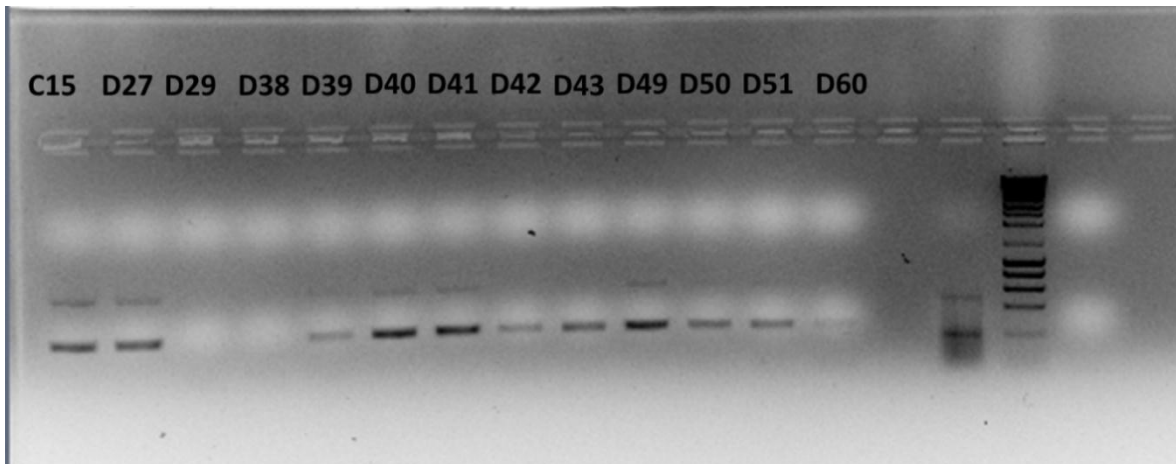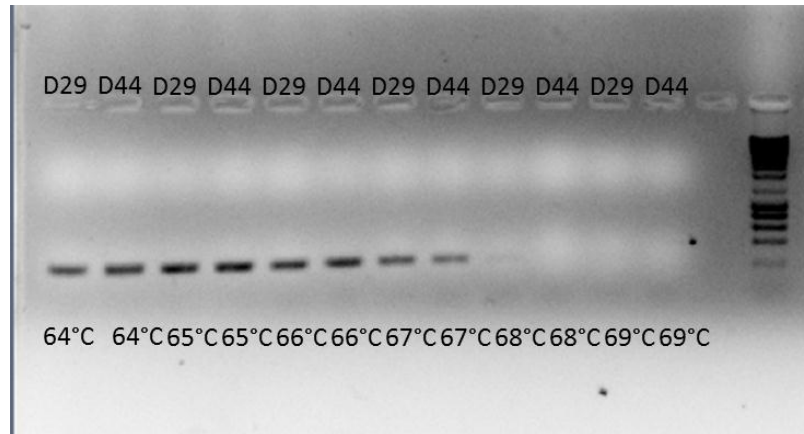

Figure 14. Representative image of the resulting bands obtained from the amplification of the 3'UTR of the ApoE gene in 13 samples, using ApoE primer pair 3 and an annealing temperature of 59°C.

In order to avoid this problem, a new annealing temperature gradient was performed ranging from 59°C to 69°C.

MiRNA contribution to APP metabolism and Aβ production in Alzheimer's disease:
Identification of new miRNA-related SNPs in the 3'UTR of human APP and APOE genes

37

Figure 15. Representative image of the resulting bands obtained from a second optimization of the ApoE primer pair 3 at annealing temperatures ranging from 64°C to 69°C.

The resulting amplification showed complete absence of nonspecific bands and allowed to determine that 67°C was higher temperature limit for Primer pair 3 annealing.
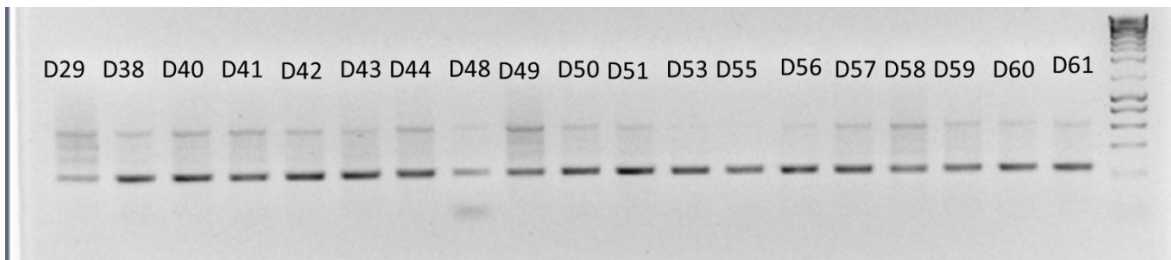

Figure 16. Representative image of the resulting bands obtained from the amplification of the 3'UTR of the ApoE gene of 19 samples using ApoE primer pair 3 and an annealing temperature of 67°C.

When performing the PCR with the annealing temperature set at 67°C, the same nonspecific amplification occurred, even in samples that have previously resulted in specific products in the same conditions, such as D29 and D44.

Since we were not able to devise alternative PCR conditions to this set of primers that would allow specific amplification for all samples, only samples that exhibited specific amplification under the latter conditions were submitted for sequencing.

MiRNA contribution to APP metabolism and Aβ production in Alzheimer's disease:
Identification of new miRNA-related SNPs in the 3'UTR of human APP and APOE genes

38

4.2 APP 3'UTR sequencing and SNP detection

Following 3'UTR amplification, all PCR products were purified and sequenced.

All the sequences obtained from the control group for both the App and ApoE perfectly matched the documented 3'UTR sequences present on the NCBI and ENSEMBLE databases.

Regarding the 3'UTR of the APP gene, a total of 9 potential heterozygous SNPs were detected in 2 samples from group 3 (with 3 of them being common between samples) and 1 potential heterozygous SNP was detected in 1 sample from group 2.

The App 3'UTR sequencing of subject D43 resulted in the detection of 6 potential heterozygous SNPs. The localization and nucleotide substitutions of this subject were as follows: G16T (figure 18), G28A (figure 18), T43A (figure 19), C95A (figure 22), A1079C (figure 21) and G1116C (figure 22).
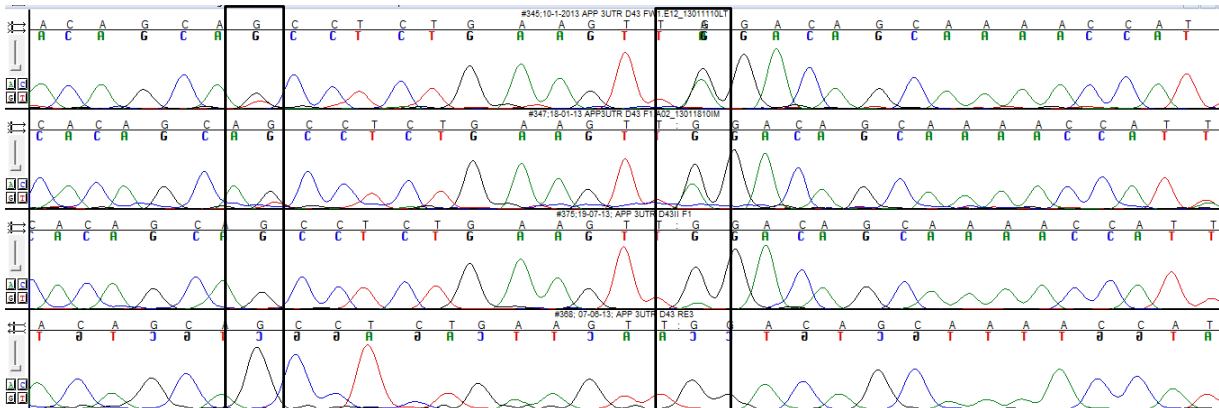

Figure 18. SNP detection via chromatographic analysis on the SEQUENCHER software. The two top rows represent a fragment of the obtained sequence from D43 sequencing using primer Fw1 (duplicates). Locations of peak overlaps are framed by black lines. Guanine 16 shows an overlap with thymine and Guanine 18 shows an overlap with Adenine. The chromatogram of the third row was obtained using primer Fw1 on a new PCR product of D43's App 3'UTR and the chromatogram on the fourth row was obtained using primer Re 3 as means of SNP confirmation. No peak overlap was observed on the third and fourth rows.
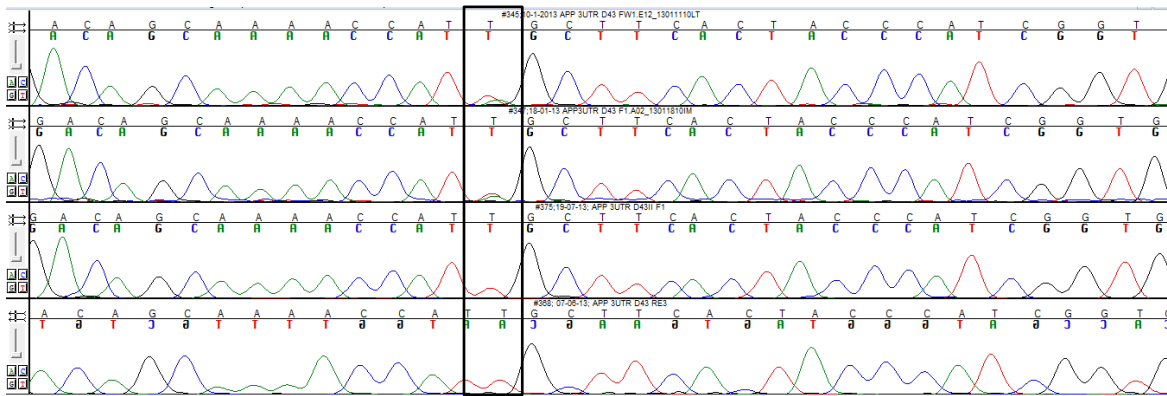
MiRNA contribution to APP metabolism and Aβ production in Alzheimer's disease: Identification of new miRNA-related SNPs in the 3'UTR of human APP and APOE genes

39

Figure 19. SNP detection via chromatographic analysis on the SEQUENCHER software. The two top rows represent a fragment of the obtained sequence from D43 sequencing using primer Fw1 (duplicates). Locations of peak overlaps are framed by black lines. Thymine 43 shows an overlap with adenine. The chromatogram of the third row was obtained using primer Fw1 on a new PCR product of D43's App 3'UTR and the chromatogram on the fourth row was obtained using primer Re 3 in order to perform SNP confirmation. No peak overlap was observed in the third and fourth rows.
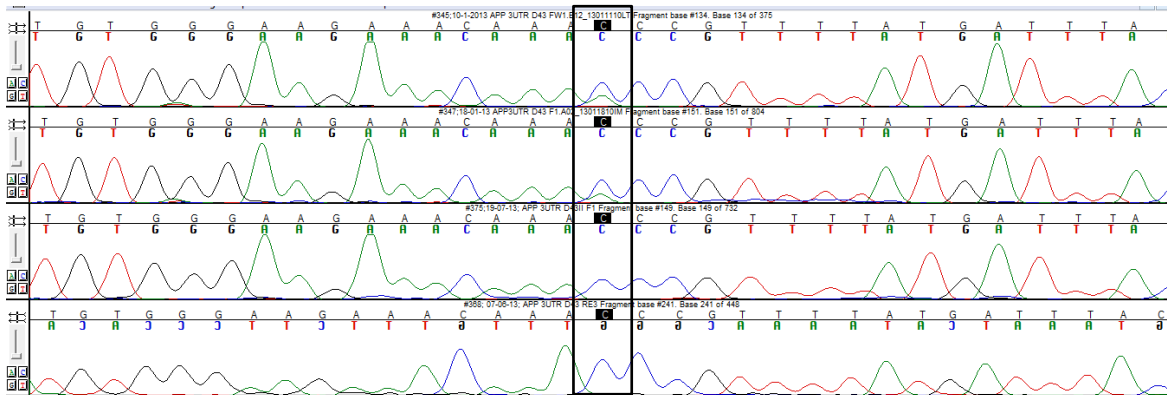

Figure 20. SNP detection via chromatographic analysis on the SEQUENCHER software. The two top rows represent a fragment of the obtained sequence from D43 sequencing using primer Fw1 (duplicates). Locations of peak overlaps are framed by black lines. Cytosine 95 shows an overlap with adenine. The chromatogram of the third row was obtained using primer Fw1 on a new PCR product of D43's App 3'UTR and the chromatogram on the fourth row was obtained using primer Re 3 in order to perform SNP confirmation. No peak overlap was observed on the third and fourth rows.
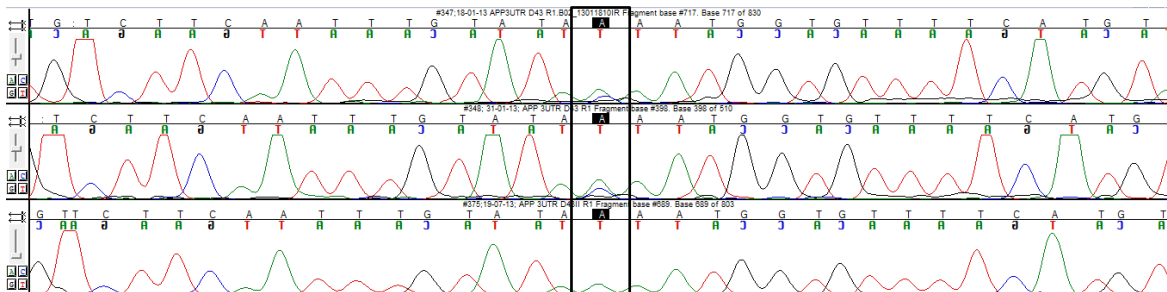

Figure 21. SNP detection via chromatographic analysis on the SEQUENCHER software. The two top rows represent a fragment of the obtained sequence from D43 sequencing using primer Re1 (duplicates). Locations of peak overlaps are framed by black lines. Adenine 1079 shows an overlap with cytosine. The chromatogram of the third row was obtained using primer Re1 on a new PCR product of D43's App 3'UTR in order to perform SNP confirmation and no peak overlap was observed..
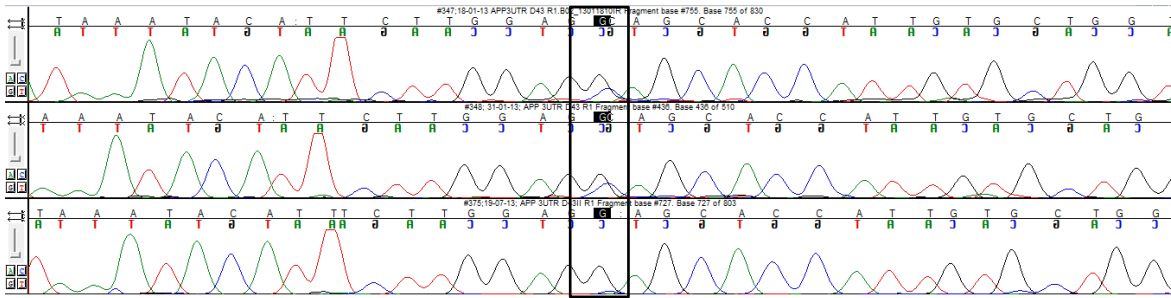
Figure 22. SNP detection via chromatographic analysis on the SEQUENCHER software. The two top rows represent a fragment of the obtained sequence from D43 sequencing using primer Re1 (duplicates). Locations of peak overlaps are framed by black lines. Guanine 1116 shows an overlap with cytosine. The chromatogram of the third row was obtained using primer Re1 on a new PCR product of D43's App 3'UTR in order to perform SNP confirmation and no peak overlap was observed.

Subject D47 showed a total of 3 potential heterozygous SNP's: C (figure 23), C95A (figure 24) and G1116C (figure 25), all common to subject D43.
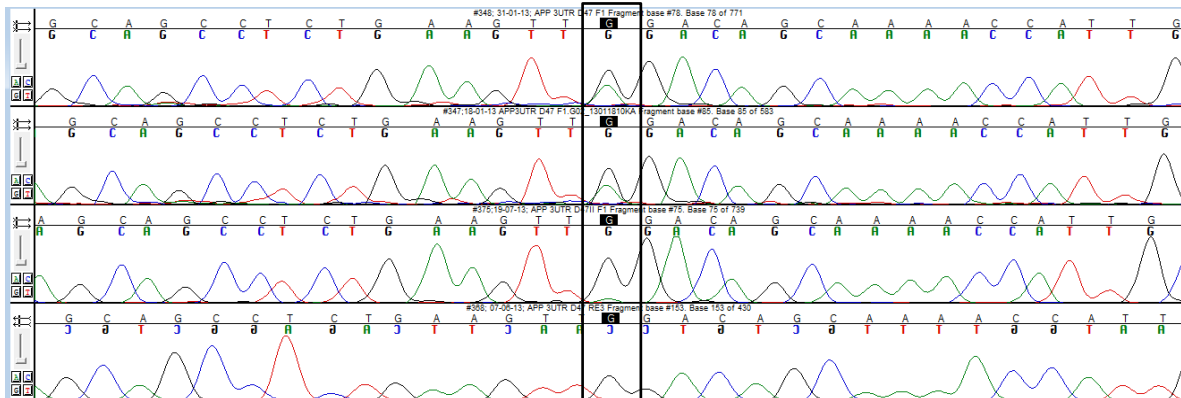

Figure 23. SNP detection via chromatographic analysis on the SEQUENCHER software. The two top rows represent a fragment of the obtained sequence from D47 sequencing using primer Fw1 (duplicates). Locations of peak overlaps are framed by black lines. Guanine 28 shows an overlap with adenine. The chromatogram of the third row was obtained using primer Fw1 on a new PCR product of D43's App 3'UTR and the chromatogram on the fourth row was obtained using primer Re 3 in order to perform SNP confirmation. No peak overlap was observed on the third and fourth rows.

MiRNA contribution to APP metabolism and Aβ production in Alzheimer's disease:
Identification of new miRNA-related SNPs in the 3'UTR of human APP and APOE genes

Figure 24. SNP detection via chromatographic analysis on the SEQUENCHER software. The two top rows represent a fragment of the obtained sequence from D47 sequencing using primer Fw1 (duplicates). Locations of peak overlaps are framed by black lines Cytosine 95 shows an overlap with adenine. The chromatogram of the third row was obtained using primer Fw1 on a new PCR product of D43's App 3'UTR and the chromatogram on the fourth row was obtained using primer Re 3 in order to perform SNP confirmation. No peak overlap was observed on the third and fourth rows.
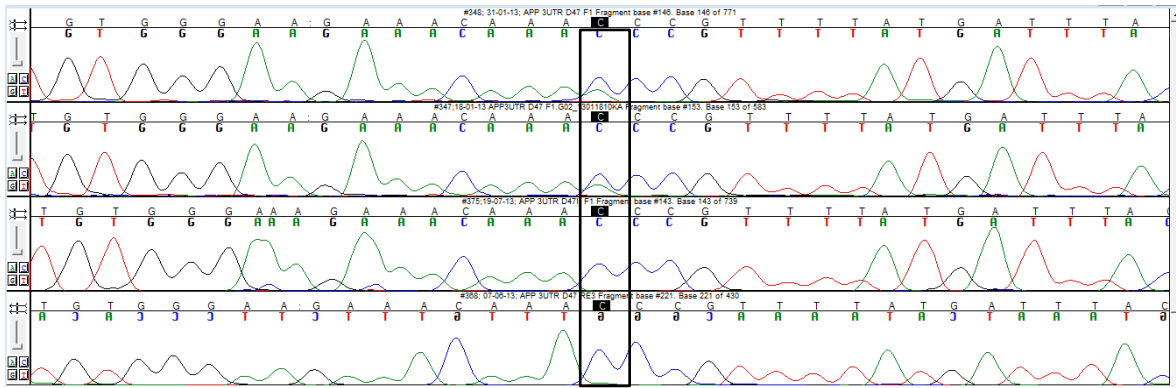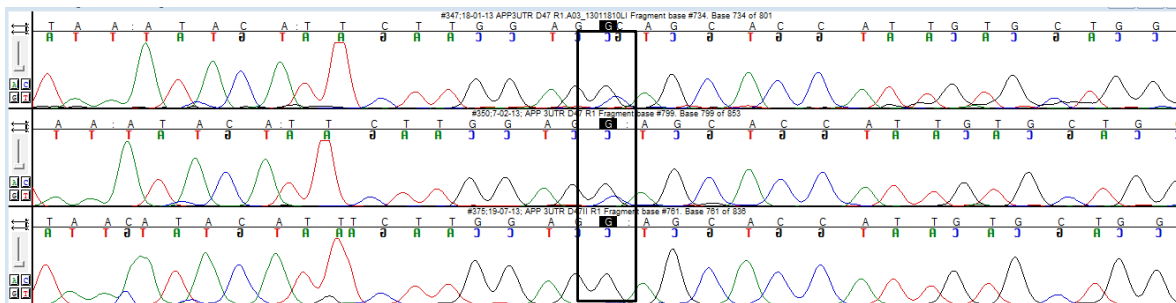

Figure 25. SNP detection via chromatographic analysis on the SEQUENCHER software. The two top rows represent a fragment of the obtained sequence from D47 sequencing using primer Re1 (duplicates). Locations of peak overlaps are framed by black lines. Guanine 1116 shows an overlap with cytosine. The chromatogram of the third row was obtained using primer Re1 on a new PCR product of D43's App 3'UTR in order to performSNP confirmation and no peak overlap was observed.

In order to be confirmed as a SNP, a specific nucleotide change must be detected in the two independent PCR products and the peak overlap must be concordant. Furthermore, the mismatch location should exhibit similar peak overlap in both forward and reverse sequence reads.

In order to validate the observed mismatches as SNPs, two additional primers were designed, since all the hypothetical mismatches detected on D43 and D47 were only covered by either the Fw1 primer or the Re1 primer

MiRNA contribution to APP metabolism and Aβ production in Alzheimer's disease:
Identification of new miRNA-related SNPs in the 3'UTR of human APP and APOE genes

42

App 3'UTR Fw3

	Sequence (5'->3')	Template strand	Length	Tm	GC%
Forward primer	GGTGCTCTGCTGGTCTTCAA	Plus	20	60.25	55.00

App 3'UTR Re3

	Sequence (5'->3')	Template strand	Length	Tm	GC%
Reverse primer	ACTGGCTAAGGGGCTATGTG	Minus	20	59.16	55.00

Figure 26. Primers Fw3 and Re3, used in the sequencing of App 3'UTR for SNP validation. Primer Fw3 was designed to provide a complementary sequence read to the primer Re1. Primer Re3 was designed to provide a complementary sequence read to the primer Fw1.

The chromatographic results obtained from the confirmation assays, which consisted in re-sequencing with new PCR products and sequencing with primers Fw3 and Re3, showed no nucleotide overlaps in the locations previously hypothesized to bear heterozygous SNPs.

However, the App 3'UTR sequencing of subject D39 resulted in the detection of another potential heterozygous SNP. A peak overlap of thymine and cytosine was detected in the position 310 of the 3'UTR when both primer Fw1 and Re2 were used. Further confirmation was achieved when a new PCR reaction and re-sequencing was performed, and provided concordant results, therefore validating this mismatch as a new SNP.
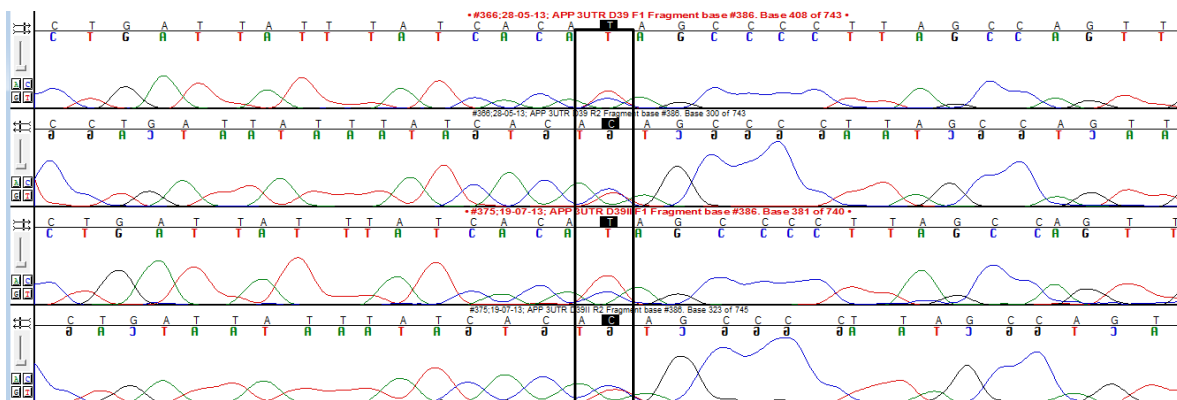

Figure 27. SNP detection via chromatographic analysis on the SEQUENCHER software. The two top rows represent a fragment of the obtained sequence from D39 sequencing using the primers Fw1 and Re2. Locations of peak overlaps are framed by black lines. Thymine 310 shows an overlap with cytosine. The chromatograms of the third and fourth row were obtaining using primers Fw1 and Re2 on a new PCR product of D39's App 3'UTR as means of SNP confirmation. The cytosine peak remained coincident with the peak for thymine 310.

MiRNA contribution to APP metabolism and Aβ production in Alzheimer's disease:
Identification of new miRNA-related SNPs in the 3'UTR of human APP and APOE genes

4.3 APP 3'UTR sequencing

Sequencing of 3'UTR of ApoE was successfully performed on 4 control samples, 7 samples from group 2 and 14 samples from group 3. All the obtained sequences perfectly matched the 3'UTR sequence displayed on both NCBI and ENSEMBLE, showing no evidence of the existence of mismatched SNPs (figure 28).
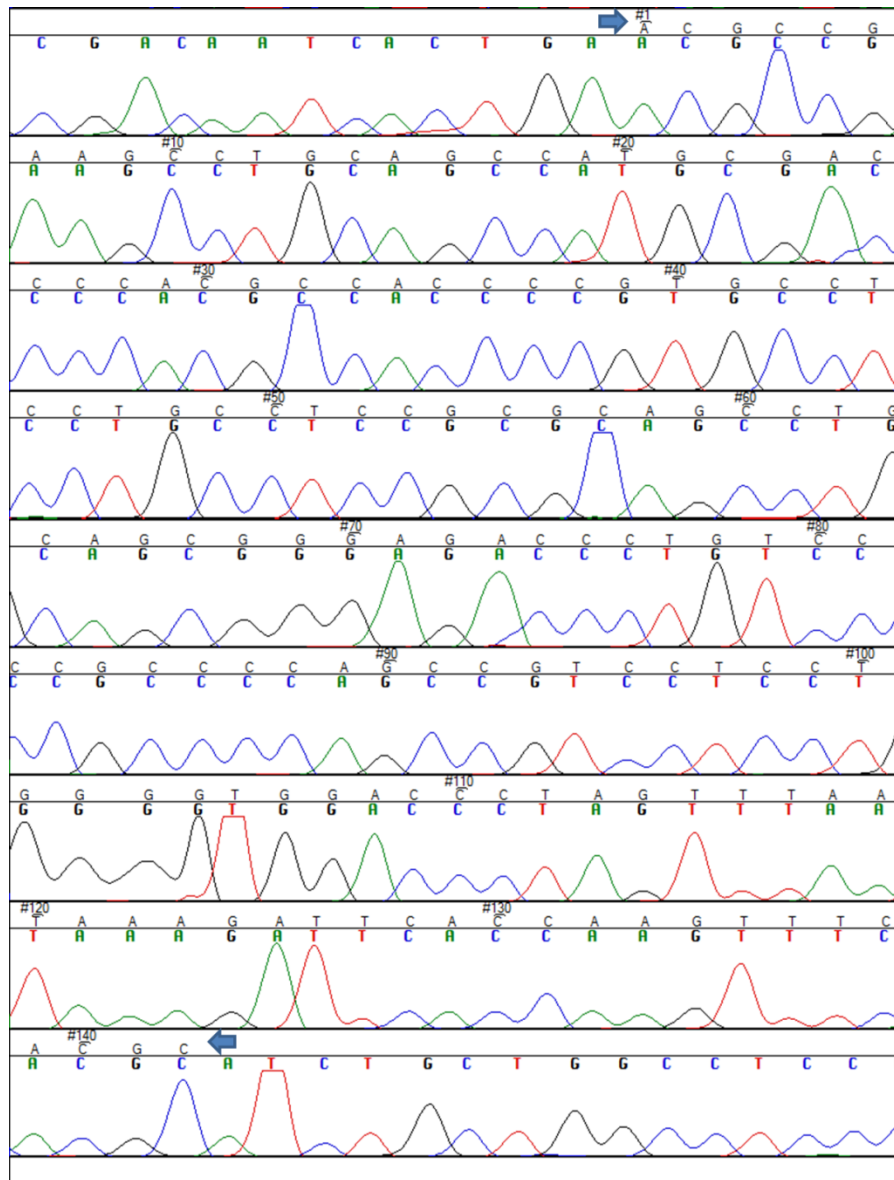

Figure 17. Representative chromatographic analysis of the 3'UTR sequence of the ApoE gene using the SEQUENCHER software. The sequence was obtained using the primer Fw3 from the ApoE 3'UTR primer pair 3 set. The sequence of the 3'UTR is delimited by the two blue arrows. This particular sequence was obtained from D42.

MiRNA contribution to APP metabolism and Aβ production in Alzheimer's disease: Identification of new miRNA-related SNPs in the 3'UTR of human APP and APOE genes

44

4.4 Prediction of SNP effects on miRNA function

The possible influence of the detected mismatches on miRNA binding to the 3'UTR of APP was determined by comparing the Watson-Crick base-pairing, predicted by microRNA.org database, between the App 3'UTR and miRNA sequences in both the presence of a SNP or in the standard alignment.

The microRNA.org database analysis highlighted 6 miRNAs whose base pairing could likely be affected in the presence of a T → C polymorphism in the position 310 of the 3'UTR of APP.

Figure 29. miRNAs predicted to bind in the vicinity of nucleotide 310 of the 3'UTR sequence of APP mRNA. The underlined nucleotide corresponds to the location of the detected T360C polymorphism. A green underline indicates that the SNP creates a Watson-Crick base pairing and a red underline signifies that the detected SNP compromises a Watson-Crick base pairing.

MiRNA contribution to APP metabolism and Aβ production in Alzheimer's disease:
Identification of new miRNA-related SNPs in the 3'UTR of human APP and APOE genes

45

Although the validation results did not allow the consideration of the G16T substitution present in D43 as a valid SNP, the bioinformatic analysis highlighted this segment of the App 3'UTR as target for the higly conserverd has-miR-485-5p.

hsa-miR-485-5p/APP Alignment

```
3' cuuaaGUAGUGCCGGUCGGAGa 5' hsa-miR-485-5p
        |: ||| | ||||||||
1:5' accccCGCCACAG-CAGCCUCu 3' APP
```

mirSVR score: -0.4481
PhastCons score: 0.7586

Figure 30. Predicted alignment of miR-485-5p to the 3'UTR sequence of APP mRNA. The nucleotide underlined in red represents the location of the detected artifact in the first chromatograms of D43. If the artifact was validated as a SNP, its presence would impair the affinity of miRNA-485-5p towards the 3'UTR of APP miRNA.

Since the binding of mir-485-5p to the 3'UTR of APP was predicted by several bioinformatics tools but was not, until the date, experimentally validated, we decided to perform a luciferase validation assay for this miRNA.

MiRNA contribution to APP metabolism and Aβ production in Alzheimer's disease:
Identification of new miRNA-related SNPs in the 3'UTR of human APP and APOE genes

46

4.5 MiRNA target validation

HEK 293T cells transfected simultaneously with the APP 3'UTR reporter plasmid (p3UTR) and the miRNA-485-5p expression plasmid exhibited a 49% decrease in luciferase activity with respect to the luciferase activity observed in the same cell line following transfection with p3UTR and a control plasmid encoding GFP. These results suggest that miR-485-5p is able to specifically bind to the 3'UTR of the APP mRNA, limiting the production of the luciferase protein.
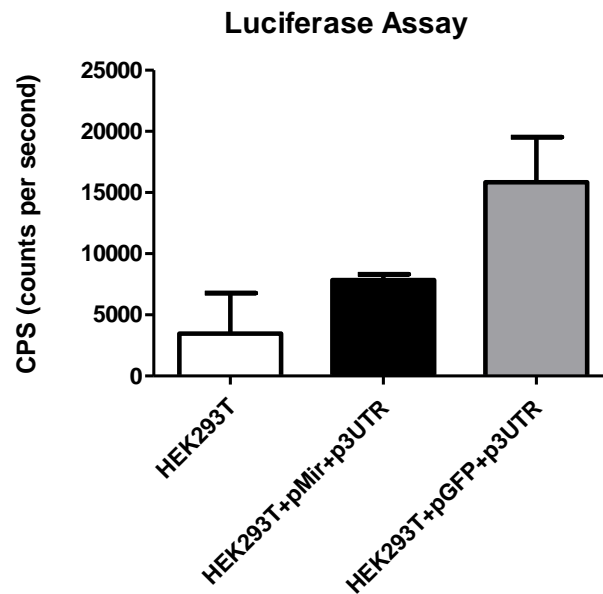

Figure 31. Measurement of luciferase activity following HEK293T cell transfection. Hek293T cells were counted and plated one day before transfection with two distinct plasmid mixes. The cells received 1µg of pMir-485-5p and 1µg of APP 3'UTR reporter plasmid (p3UTR) or 1µg of pGFP and 1µg of APP 3'UTR reporter plasmid (p3UTR) complexed with the Lipofectamine LX transfection reagent. Transfection was performed during 4 hours. After this period the cells were washed and incubated for 48h with normal medium. Luciferase activity was measured in the cellular lysates following addition of ATP and luciferin. Luciferase activity is presented as CPS (counts per second) for the negative control (untransfected HEK293T) and for both plasmids mixes (HEK293T+pMir+p3UTR and HEK293T+pGFP+p3UTR). Results are representative of a single experiment with each condition performed in triplicate.

MiRNA contribution to APP metabolism and Aβ production in Alzheimer's disease:
Identification of new miRNA-related SNPs in the 3'UTR of human APP and APOE genes

47

Discussion

MiRNA contribution to APP metabolism and Aβ production in Alzheimer's disease:
Identification of new miRNA-related SNPs in the 3'UTR of human APP and APOE genes

48

5. Discussion

Ninety-five percentof all AD patients present the sporadic form of the disease, indicating that the large majority of AD casesare triggered by unknown causes. Currently, the only factor known to trigger AD is an increased gene dosage, which is found in only 5% of all AD patients and can have several genetic causes (familial AD).

Over 500 genes have been proposed to detain AD ethiopathogenic relevance in the presence of genetic polymorphisms. In addition, several studies have shown that miRNA levels are deregulated in AD patients. In fact, a recent study was able to distinguish AD and control subjects with 93% accuracy trough miRNA profiling alone [48].

With this in mind, we focused this project on revisiting the relevance of protein expression deregulation in AD in the presence of miRNA-related SNPs , aiming at taking part in the exploratory effort required to fully uncover the relevance of miRNAs in this multifactorial neuropathology.

The last study to adress the influence of SNPs on miRNA binding, in the context of AD, was published in 2008. This study presented four specific SNPs detected in the 3'UTR region of APP and seven specific SNPs detected in the 3'UTR region of BACE1 in AD ptients. However, the detected polymorphisms were reported as non-determinant for miRNA binding affinity and, therefore, of no major relevance for AD progression [49].

In 2011, Delay et al. set out to determine if the previously reported SNPs could, in fact, modulate miRNA function. This author was able to demonstrate that two of the previously overlooked SNPs could influence the binding of miRNA-147 and miRNA-20a to the APP 3'UTR.

In this project, we were able to successfully sequence the 3'UTR of the APP gene in 12 healthy controls, 25 AD patients and 18 patients with MCI. The inclusion of an MCI group was made since it is assumed that the vast majority of these patients will develop AD.

Our results culminated in the validation of one MCI patient-specific heterozygous SNP, on patient D39, which consisted in the nucleotide substitution of T → C in the position 310 of the 3'UTR of APP. The bioinformatic analysis of this SNP highlighted five possible miRNAs whose function would likely be altered due to this base-pairing change: MiRNA-582-3p, miRNA-423-5p, miRNA-185*, miRNA-31* and miRNA-892b.

MiRNA contribution to APP metabolism and Aβ production in Alzheimer's disease:
Identification of new miRNA-related SNPs in the 3'UTR of human APP and APOE genes

49

Four of this miRNAs (miRNA-582-3p, miRNA-423-5p, miRNA-185*, and miRNA-892b) were predicted to gain higher complementarity to the 3'UTR of the APP gene due to the presence of this polymorphism. The physiological relevance of such higher affinity was, however, predicted to be of no major significance since the nucleotide substitution provided an extra base pairing at a position outside of the seed region of miRNA-582-3p and miRNA-892b. As for miRNA-423-5p and miRNA-185*, the nucleotide substitution permuted an existent non-Watson-Crick base pairing between the uracil present at the mRNA of the APP and the guanine present at the miRNA to a Watson-Crick base pairing of cytosine and guanine which presents higher thermodynamic stability. However, these changes were located outside of the seed region of both miRNAs and, therefore, their contribution to the overall binding affinity of the miRNAs towards the APP mRNA is limited.

Regarding miRNA-31*, this polymorphism was predicted to compromise the miRNA complementarity with the APP mRNA since it affects base pairing within the seed region. It would be interesting to assess the impact that the complementarity hindrance created by this SPN could have on APP translation and its contribution to the development of mild cognitive impairment and to a possible progression to AD. MiRNA-31* was already demonstrated to be physiologically relevant in the context of Oral Leukoplakia [50] and could, therefore, provide some degree of regulation of the APP protein.

During the progress of our study, several other SNP candidates were detected (figure 31) but were considered to be false-positives due to the presence of non-concordant peak overlaps in the chromatographic analysis. However, one of these potential SNPs, was particularly interesting, taken into consideration the influence that one highly conserved miRNA, miRNA-485-5p , predicted to bind to 3'UTR region were the mismatch was located, could have on the regulation of APP. MiRNA-485-5p has already been shown to be downregulated in AD and was validated as strong regulator of BACE1, one of the key proteins involved in AD [51].

We determined the possible influence of miRNA-485-5p on APP expression by simultaneously transfecting HEK293T cells with a miRNA-458-5p expressing plasmid and with a APP 3'UTR luciferase reporter plasmid, were the luciferase gene is under the control of the same promoter of the 3'UTR. This procedure assessed the degree of posttranscriptional regulation that this miRNA can have on APP. Our results showed that in the absence of the miRNA-458-5p expressing plasmid, the transfected cells yielded a decrease of 61% in luciferase activity with respect to cells transfected with the 3'UTR plasmid and a control plasmid encoding GFP. Since the

MiRNA contribution to APP metabolism and Aβ production in Alzheimer's disease: Identification of new miRNA-related SNPs in the 3'UTR of human APP and APOE genes

50

total luciferase activity is proportional to the amount of expressed luciferase, these results provided compelling evidence that miRNA-485-5p is able to bind to the 3'UTR of the APP gene and regulate APP translation.
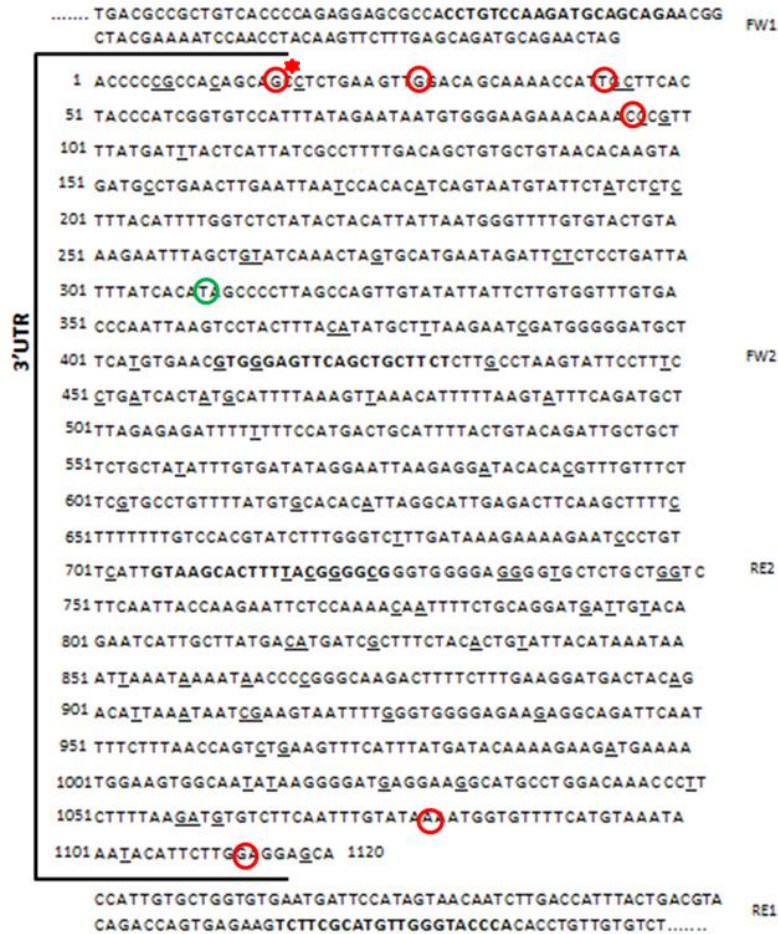

Figure 31. Overview of the location of the artifact signals and the validated SNP detected in this study in the 3'UTR sequence of the APP gene.. The primer sequences are highlighted in bold. Each of the red circular frames represents the location of one of the peak artifacts and the green circular frame represents the location of the validated T360C heterozygotic polymorphism. The frame marked with the asterisk highlights the location of miRNA-485-5p binding.

Our results from ApoE 3'UTR sequencing did not provide any evidence of existing SNPs and were fairly limited due to the number of sequencing-usable samples. The discrepancy observed in the PCR product specificity obtained in different PCR reactions for the same samples excludes that the specific amplification failure might be due to inherent characteristics of the genome of each subject. The PCR conditions were replicated in three different thermocyclers and unspecific amplification occurred even when new aliquots of reaction buffer, DNA polymerase, $MgCl_2$, H_2O, dNTP's and primers were used for the master mix.

MiRNA contribution to APP metabolism and Aβ production in Alzheimer's disease: Identification of new miRNA-related SNPs in the 3'UTR of human APP and APOE genes

51

Conclusions and future Perspectives

6. Conclusions and future perspectives

Given the exploratory nature of this project, the obtained results were not sufficient to determine whether SNPs in the 3'UTR region of the APP and ApoE genes are playing a significant role on AD ethiopathology.

There is a possibility that the detected SNP on D39 could in fact result in a diminished translational inhibition of the mRNA of APP, contributing to the escalation of the diagnosed cognitive impairment. This possibility could promptly be tested trough the previously described transfection and luciferase assays. It would also be interesting to accompany the symptomatic development of this patient in order to determine if this polymorphism could drive the full installment of AD.

The significance of SNPs influence on miRNA function in the AD context can still arise from other genes strongly related to this pathology. BACE1 and PSEN-1 are prime examples of such genes that couldn not be approached on this study due to the extensive length of their 3'UTR regions comprising 3865nt and 4401nt, respectively. Next-generation sequencing is likely the best approach to tackle such lengthy sequences and further elucidate the true impact that genetic variability can have on AD.

To the best of our knowledge, this is the first time that miRNA-485-5p binding to the APP 3'UTR has been validated experimentally. We strongly believe that, in light of the strong pairing between miRNA-485-5p and the APP mRNA, the upregulation of this miRNA in the brain tissue could contribute to the decrease of APP expression, constituting an interesting new therapeutic strategy for Alzheimer's disease.

MiRNA contribution to APP metabolism and Aβ production in Alzheimer's disease:
Identification of new miRNA-related SNPs in the 3'UTR of human APP and APOE genes

53

References

1. Xu, W., Ferrari, C. & Wang, H.-X. *Epidemiology of Alzheimer's Disease*, (2013).
2. Prince, M. *et al.* The global prevalence of dementia: a systematic review and metaanalysis. *Alzheimers Dement* **9**, 63-75 e2 (2013).
3. Singh, S., Kushwah, A.S., Singh, R., Farswan, M. & Kaur, R. Current therapeutic strategy in Alzheimer's disease. *Eur Rev Med Pharmacol Sci* **16**, 1651-64 (2012).
4. Heneka, M.T., O'Banion, M.K., Terwel, D. & Kummer, M.P. Neuroinflammatory processes in Alzheimer's disease. *J Neural Transm* **117**, 919-47 (2010).
5. Thies, W. & Bleiler, L. 2013 Alzheimer's disease facts and figures. *Alzheimers Dement* **9**, 208-45 (2013).
6. Podtelezhnikov, A.A. *et al.* Molecular insights into the pathogenesis of Alzheimer's disease and its relationship to normal aging. *PLoS One* **6**, e29610 (2011).
7. Heneka, M.T. & O'Banion, M.K. Inflammatory processes in Alzheimer's disease. *J Neuroimmunol* **184**, 69-91 (2007).
8. Cameron, B. & Landreth, G.E. Inflammation, microglia, and Alzheimer's disease. *Neurobiol Dis* **37**, 503-9 (2010).
9. Mohamed, A., Cortez, L. & de Chaves, E.P. Aggregation state and neurotoxic properties of alzheimer beta-amyloid peptide. *Curr Protein Pept Sci* **12**, 235-57 (2011).
10. Schonrock, N. *et al.* Neuronal microRNA deregulation in response to Alzheimer's disease amyloid-beta. *PLoS One* **5**, e11070 (2010).
11. Storandt, M., Head, D., Fagan, A.M., Holtzman, D.M. & Morris, J.C. Toward a multifactorial model of Alzheimer disease. *Neurobiol Aging* (2012).
12. Storandt, M., Head, D., Fagan, A.M., Holtzman, D.M. & Morris, J.C. Toward a multifactorial model of Alzheimer disease. *Neurobiol Aging* **33**, 2262-71 (2012).
13. Fandrich, M. Oligomeric intermediates in amyloid formation: structure determination and mechanisms of toxicity. *J Mol Biol* **421**, 427-40 (2012).
14. Rodriguez, J.J., Olabarria, M., Chvatal, A. & Verkhratsky, A. Astroglia in dementia and Alzheimer's disease. *Cell Death Differ* **16**, 378-85 (2009).
15. Nagele, R.G., Wegiel, J., Venkataraman, V., Imaki, H. & Wang, K.C. Contribution of glial cells to the development of amyloid plaques in Alzheimer's disease. *Neurobiol Aging* **25**, 663-74 (2004).
16. Garwood, C.J., Pooler, A.M., Atherton, J., Hanger, D.P. & Noble, W. Astrocytes are important mediators of Abeta-induced neurotoxicity and tau phosphorylation in primary culture. *Cell Death Dis* **2**, e167 (2011).
17. Larson, M.E. & Lesne, S.E. Soluble Abeta oligomer production and toxicity. *J Neurochem* **120 Suppl 1**, 125-39 (2012).
18. Crews, L., Rockenstein, E. & Masliah, E. APP transgenic modeling of Alzheimer's disease: mechanisms of neurodegeneration and aberrant neurogenesis. *Brain Struct Funct* **214**, 111-26 (2010).
19. Selkoe, D.J. The cell biology of beta-amyloid precursor protein and presenilin in Alzheimer's disease. *Trends Cell Biol* **8**, 447-53 (1998).
20. Kuret, J. *et al.* Pathways of tau fibrillization. *Biochim Biophys Acta* **1739**, 167-78 (2005).
21. LaFerla, F.M. & Oddo, S. Alzheimer's disease: Abeta, tau and synaptic dysfunction. *Trends Mol Med* **11**, 170-6 (2005).
22. Thies, W. & Bleiler, L. 2011 Alzheimer's disease facts and figures. *Alzheimers Dement* **7**, 208-44 (2011).

MiRNA contribution to APP metabolism and Aβ production in Alzheimer's disease:
Identification of new miRNA-related SNPs in the 3'UTR of human APP and APOE genes

54

23. Hatters, D.M., Peters-Libeu, C.A. & Weisgraber, K.H. Apolipoprotein E structure: insights into function. *Trends Biochem Sci* **31**, 445-54 (2006).

24. Hauser, P.S., Narayanaswami, V. & Ryan, R.O. Apolipoprotein E: from lipid transport to neurobiology. *Prog Lipid Res* **50**, 62-74 (2011).

25. Narayanaswami, V. & Ryan, R.O. Molecular basis of exchangeable apolipoprotein function. *Biochim Biophys Acta* **1483**, 15-36 (2000).

26. Vance, J.E. & Hayashi, H. Formation and function of apolipoprotein E-containing lipoproteins in the nervous system. *Biochim Biophys Acta* **1801**, 806-18 (2010).

27. Leduc, V., Jasmin-Belanger, S. & Poirier, J. APOE and cholesterol homeostasis in Alzheimer's disease. *Trends Mol Med* **16**, 469-77 (2010).

28. Holtzman, D.M., Herz, J. & Bu, G. Apolipoprotein E and apolipoprotein E receptors: normal biology and roles in Alzheimer disease. *Cold Spring Harb Perspect Med* **2**, a006312 (2012).

29. Liu, M., Kuhel, D.G., Shen, L., Hui, D.Y. & Woods, S.C. Apolipoprotein E does not cross the blood-cerebrospinal fluid barrier, as revealed by an improved technique for sampling CSF from mice. *Am J Physiol Regul Integr Comp Physiol* **303**, R903-8 (2012).

30. Seripa, D. *et al.* The genetics of the human APOE polymorphism. *Rejuvenation Res* **14**, 491-500 (2011).

31. Grimmer, T. *et al.* Progression of cerebral amyloid load is associated with the apolipoprotein E epsilon4 genotype in Alzheimer's disease. *Biol Psychiatry* **68**, 879-84 (2010).

32. Hanson, A.J. *et al.* Effect of Apolipoprotein E Genotype and Diet on Apolipoprotein E Lipidation and Amyloid Peptides: Randomized Clinical Trial. *JAMA Neurol*, 1-9 (2013).

33. Saavedra, L., Mohamed, A., Ma, V., Kar, S. & de Chaves, E.P. Internalization of beta-amyloid peptide by primary neurons in the absence of apolipoprotein E. *J Biol Chem* **282**, 35722-32 (2007).

34. Sagare, A.P., Bell, R.D. & Zlokovic, B.V. Neurovascular dysfunction and faulty amyloid beta-peptide clearance in Alzheimer disease. *Cold Spring Harb Perspect Med* **2**(2012).

35. Brecht, W.J. *et al.* Neuron-specific apolipoprotein e4 proteolysis is associated with increased tau phosphorylation in brains of transgenic mice. *J Neurosci* **24**, 2527-34 (2004).

36. Tesseur, I. *et al.* Expression of human apolipoprotein E4 in neurons causes hyperphosphorylation of protein tau in the brains of transgenic mice. *Am J Pathol* **156**, 951-64 (2000).

37. Hoe, H.S., Freeman, J. & Rebeck, G.W. Apolipoprotein E decreases tau kinases and phospho-tau levels in primary neurons. *Mol Neurodegener* **1**, 18 (2006).

38. Almos, P.Z. *et al.* Tau haplotypes and ApoE4 do not act in synergy on Alzheimer's disease. *Psychiatry Res* **186**, 448-50 (2011).

39. Piaceri, I., Nacmias, B. & Sorbi, S. Genetics of familial and sporadic Alzheimer's disease. *Front Biosci (Elite Ed)* **5**, 167-77 (2013).

40. Delay, C., Mandemakers, W. & Hebert, S.S. MicroRNAs in Alzheimer's disease. *Neurobiol Dis* (2012).

41. Lang, M.F. & Shi, Y. Dynamic Roles of microRNAs in Neurogenesis. *Front Neurosci* **6**, 71 (2012).

42. Delay, C., Calon, F., Mathews, P. & Hebert, S.S. Alzheimer-specific variants in the 3'UTR of Amyloid precursor protein affect microRNA function. *Mol Neurodegener* **6**, 70 (2011).

43. Bushati, N. & Cohen, S.M. MicroRNAs in neurodegeneration. *Curr Opin Neurobiol* **18**, 292-6 (2008).

44. Duttagupta, R., Jiang, R., Gollub, J., Getts, R.C. & Jones, K.W. Impact of cellular miRNAs on circulating miRNA biomarker signatures. *PLoS One* **6**, e20769 (2011).

45.   Weiland, M., Gao, X.H., Zhou, L. & Mi, Q.S. Small RNAs have a large impact: Circulating microRNAs as biomarkers for human diseases. *RNA Biol* **9**(2012).

46.   Soreq, H. & Wolf, Y. NeurimmiRs: microRNAs in the neuroimmune interface. *Trends Mol Med* **17**, 548-55 (2011).

47.   Delay, C. & Hebert, S.S. MicroRNAs and Alzheimer's Disease Mouse Models: Current Insights and Future Research Avenues. *Int J Alzheimers Dis* **2011**, 894938 (2011).

48.   Leidinger, P. *et al.* A blood based 12-miRNA signature of Alzheimer disease patients. *Genome Biol* **14**, R78 (2013).

49.   Bettens, K. *et al.* APP and BACE1 miRNA genetic variability has no major role in risk for Alzheimer disease. *Hum Mutat* **30**, 1207-13 (2009).

50.   Xiao, W. *et al.* Upregulation of miR-31* is negatively associated with recurrent/newly formed oral leukoplakia. *PLoS One* **7**, e38648 (2012).

51.   Faghihi, M.A. *et al.* Evidence for natural antisense transcript-mediated inhibition of microRNA function. *Genome Biol* **11**, R56 (2010).